Variational Methods for Generating Optimal Tessellations and Their Applications

Zhonggui Chen (陈中贵)

Graphics@XMU

Computer Graphics Group
Xiamen University

http://graphics.xmu.edu.cn/~zgchen/

Outline

- Centroidal Voronoi Tessellation (CVT)
- Optimal Delaunay Triangulation (ODT)
- Capacity-constrained Centroidal Voronoi Tessellation (CapCVT)
- Centroidal Power Diagram (CPD)
- Optimal Voronoi Tessellation (OVT)
- Optimal Power Diagrams (OPD)
- Applications…



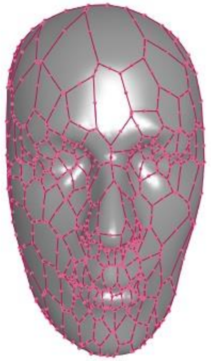
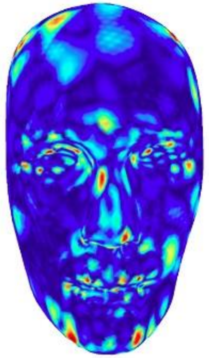
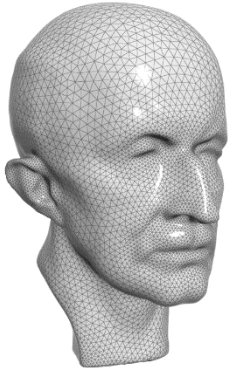

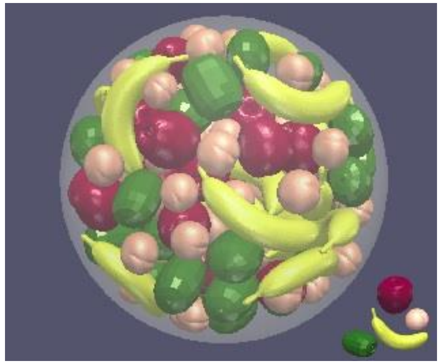

I

Centroidal Voronoi Tessellation (CVT)

Voronoi Tessellation

- **Voronoi diagram** induced by a set of points (called sites or seeds): subdivision of the plane where the faces correspond to the regions where one site is closest.
  - Let Ω be a closed region in $\mathbb{R}^n$ and $X = \{\mathbf{x}_i\}_{i=1}^N \subset \mathbb{R}^n$. For any $\mathbf{x}_i \in X$, its Voronoi cell is defined as:

$$V_i = \{\, \mathbf{x} \in \Omega, s.t. \| \mathbf{x} - \mathbf{x}_i \| \le \| \mathbf{x} - \mathbf{x}_j \|, \forall j \neq i \,\}$$

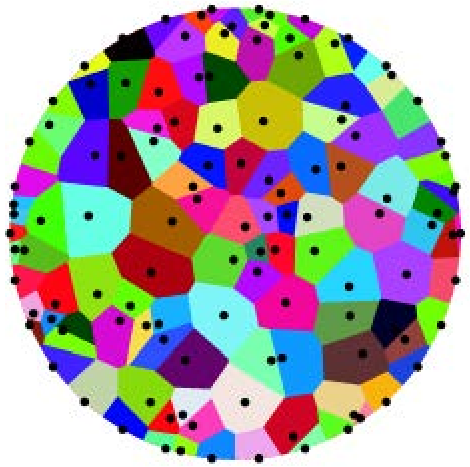

Centroidal Voronoi Tessellation

- *Definition*: A Voronoi Tessellation is a centroidal Voronoi tessellation (CVT) , if each seed coincides with the centroid of its Voronoi cell

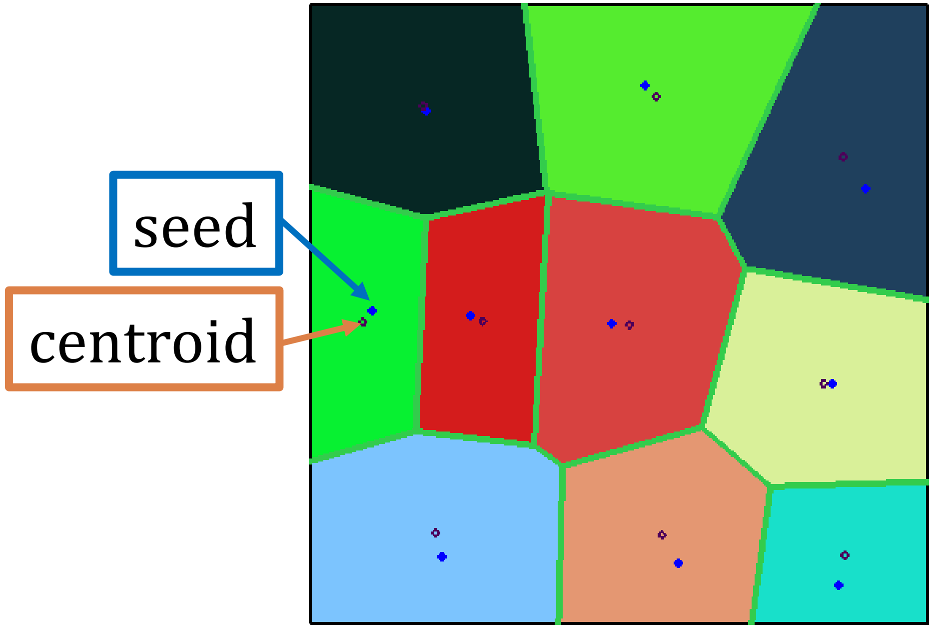

Generic VT

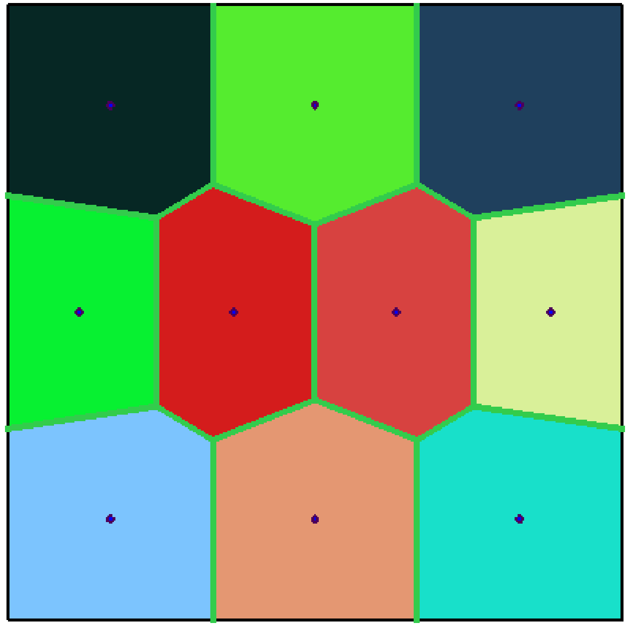

CVT

CVT Computation

- Lloyd's method [Lloyd 1982]
  1. Construct the VT $\{V_i\}_{i=1}^N$ associated with the points $\{\mathbf{x}_i\}_{i=1}^N$
  2. Compute the centroids of the Voronoi regions $\{V_i\}_{i=1}^N$; these centroids are the new set of points $\{\mathbf{x}_i\}_{i=1}^N$
  3. Check the stop criterion; if satisfied, terminate; otherwise, return to step 1

Initialization

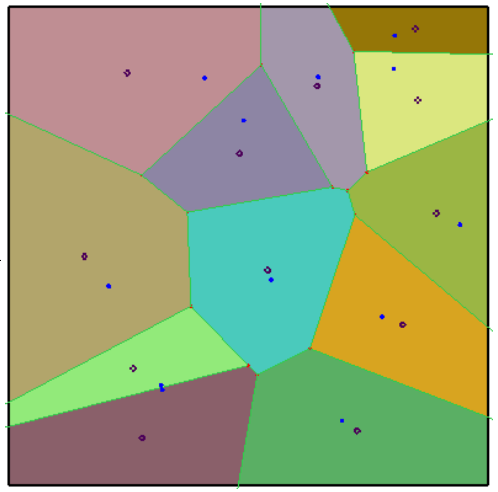

After 1 iteration

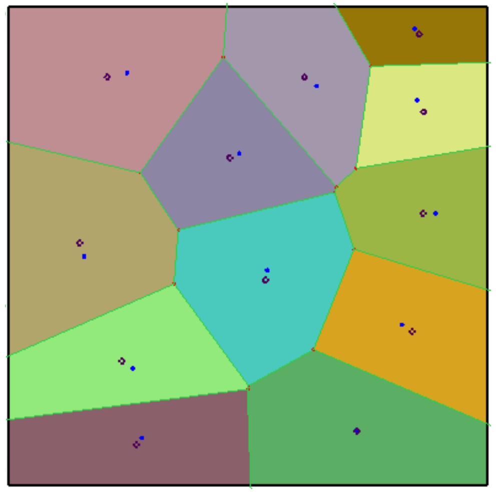

After 40 iteration

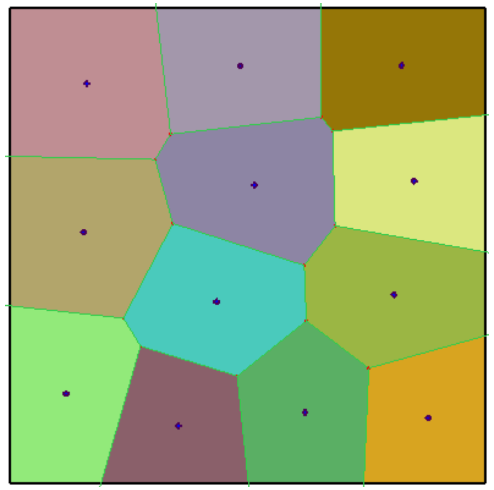

Centroidal Voronoi Tessellation

- *Definition* (Variational point of view)
  - CVT energy function:

$$\mathcal{E}_{CVT}(\mathbf{X},\mathcal{V}) = \sum_{i=1}^{n}\int_{V_i}\left\|\mathbf{x}-\mathbf{x}_i\right\|^2 d\mathbf{x} = \sum_{i=1}^{n}\int_{V_i}\left(\mathbf{x}^2 - \left(2\mathbf{x}_i^T\mathbf{x}-\mathbf{x}_i^2\right)\right)d\mathbf{x}$$

- Geometric interpretation

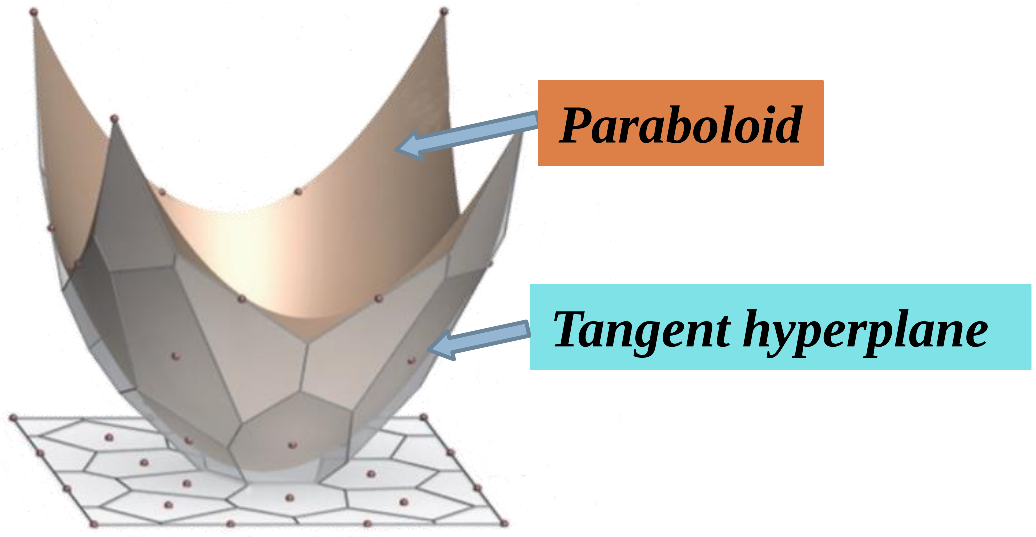

Fast Computation of CVT

- CVT function is C^2 in a **convex** domain in 2D and 3D [Liu et al. 2009]
- Newton method: quadratic convergence, too costly to compute inverse Hessian for large *n*
- BFGS method: **super-linear convergence** if *F(**X**)* is C^2 [Nocedal and Wright 1999]
- L-BFGS method: use only recent gradients to approximate inverse Hessian, low memory cost [Liu and Nocedal 1989]

Lloyd vs. L-BFSG

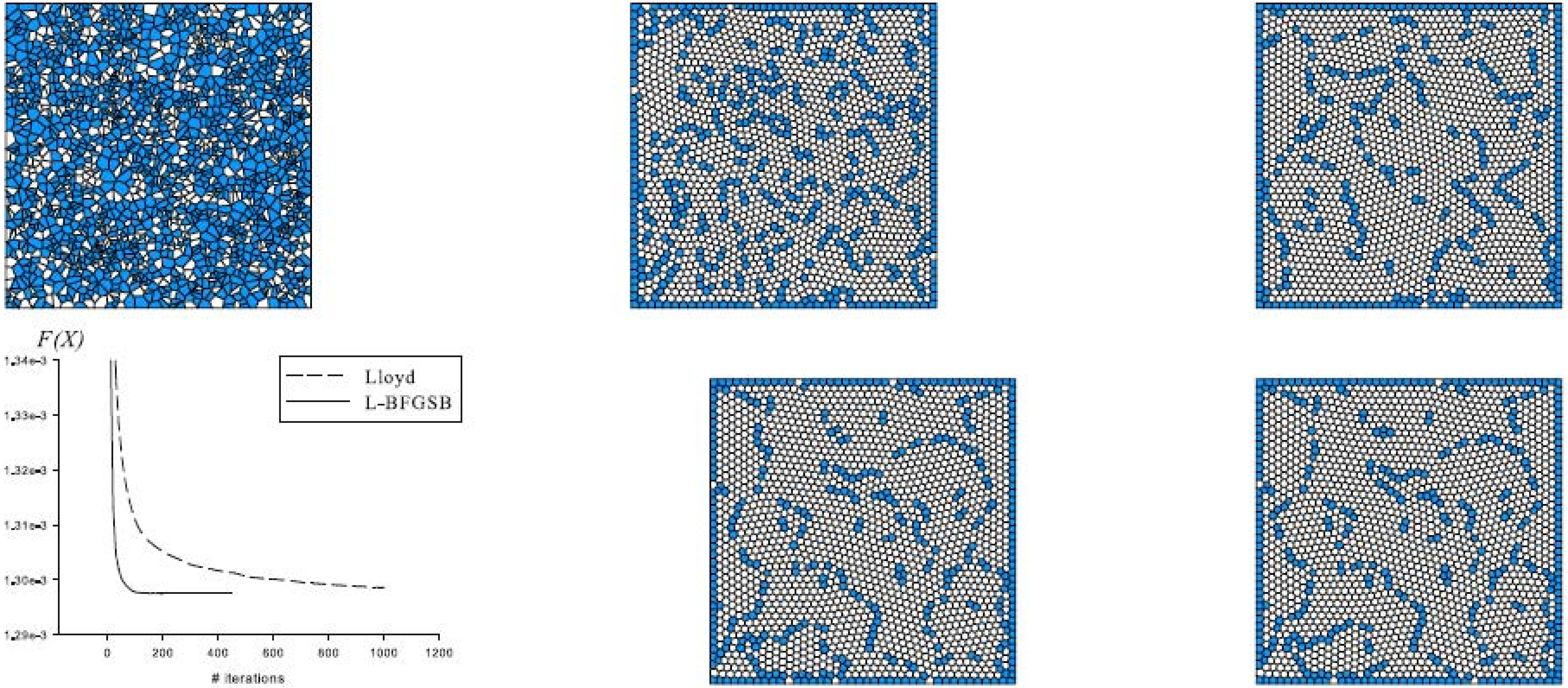

Fist row: (left) Initial Voronoi tessellation; (middle) after 100 Lloyd iterations; (right) after 1000 Lloyd iterations. **Second row**: (1): F(**X**) vs # of iterations; (2) after 100 iterations by L-BFGSB; (3) after 1000 iterations by L-BFGSB [Liu et al. 2009]

II Optimal Delaunay Triangulation (ODT)

Zhonggui Chen, Wenping Wang, Bruno Lévy, Ligang Liu, Feng Sun. ***Revisiting Optimal Delaunay Triangulation for 3D Graded Mesh Generation***. *SIAM Journal on Scientific Computing*, 36(3), A930-A954, 2014

Optimal Delaunay Triangulation (ODT)

- ODT energy function [L. Chen et al, 2004]:

$$E(X) = \|f - f_{I,\mathcal{T}}\|_{L^1(\Omega)}$$
$$= \sum_{\tau \in \mathcal{T}} \int_{\tau} f_I(\mathbf{x}) d\mathbf{x} - \int_{\Omega} f(\mathbf{x}) d\mathbf{x}$$

where $X = \{\mathbf{x}_i\}_{i=1}^{N}$ is the set of seed points, $f(\mathbf{x}) = \|\mathbf{x}\|^2$, and $f_{I,\mathcal{T}}(\mathbf{x})$ is the linear interpolation of $f(\mathbf{x})$ based on the DT $\mathcal{T}$ of a domain Ω

- ODT is defined as the global minimizer of $E(X)$ *[Chen et al, 2004]*

Optimal Delaunay Triangulation (ODT)

- ODT energy function [L. Chen et al, 2004]:

$$E(X) = \|f - f_{I,\mathcal{T}}\|_{L^1(\Omega)}$$
$$= \sum_{\tau \in \mathcal{T}} \int_{\tau} f_I(\mathbf{x}) d\mathbf{x} - \int_{\Omega} f(\mathbf{x}) d\mathbf{x}$$

Volume between the lift-up of DT and the paraboloid

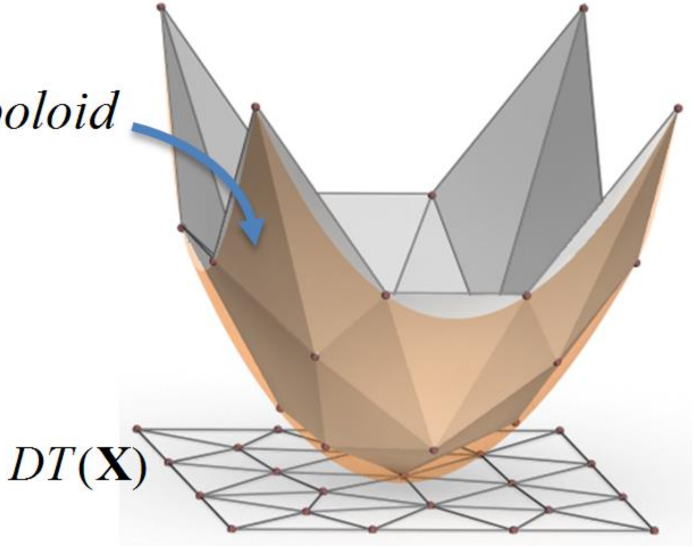

ODT Optimization

- AVV(*averaged Voronoi vertex*) method
  - (connectivity update) Compute the DT of the current vertices;
  - (position update) Move the current vertex to

$$\bar{\mathbf{x}}_i = \frac{1}{|\Omega_i|} \sum_{\tau_j \in \Omega_i} |\tau_j| \mathbf{c}_j$$

where $\mathbf{c}_j$ is the circum-center of the triangle Ω_i in the 1-ring neighborhood τ_j of the vertex $\mathbf{x}_i$.

CVT & ODT Energies

- CVT energy

$$E_{CVT}(\mathbf{X},\mathcal{V}) = \sum_{i=1}^{n}\int_{V_i}\|\mathbf{x}-\mathbf{x}_i\|^2 \mathrm{d}\mathbf{x} = \sum_{i=1}^{n}\int_{V_i}\left(\mathbf{x}^2 - \left(2\mathbf{x}_i^T\mathbf{x}-\mathbf{x}_i^2\right)\right)\mathrm{d}\mathbf{x}$$

- ODT energy

$$E(X) = \sum_{\tau\in\mathcal{T}}\int_{\tau} f_I(\mathbf{x})d\mathbf{x} - \int_{\Omega} f(\mathbf{x})d\mathbf{x}$$

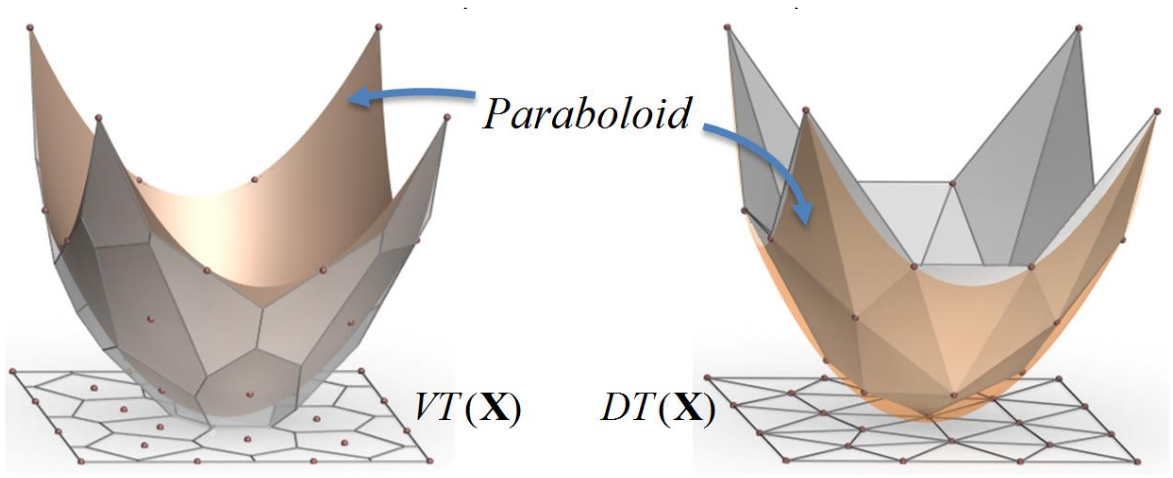

Energy Smoothness

- ODT function only has C^0 continuity *

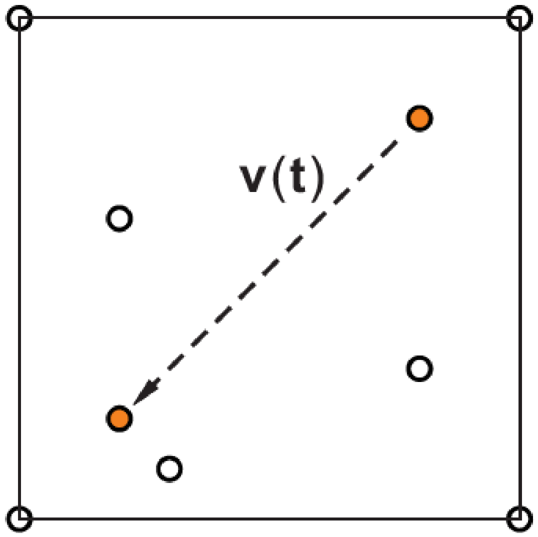

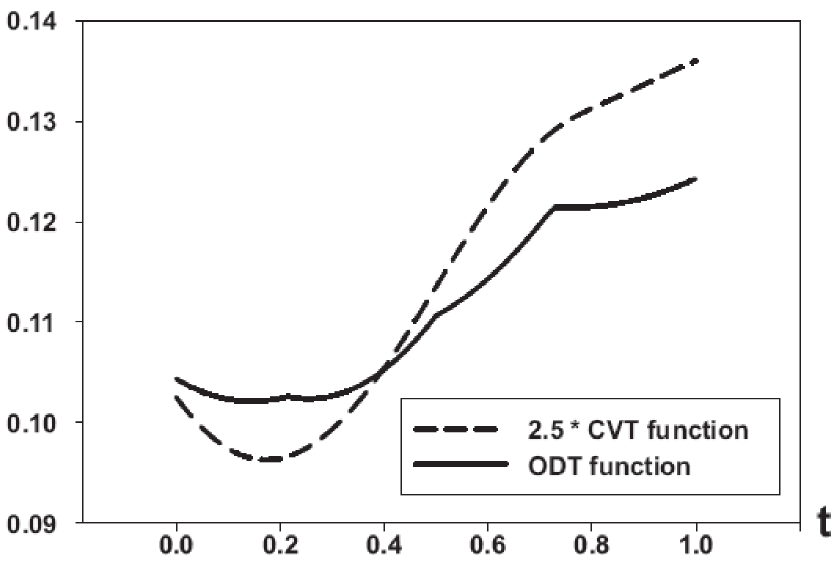

CVT vs. ODT (1)

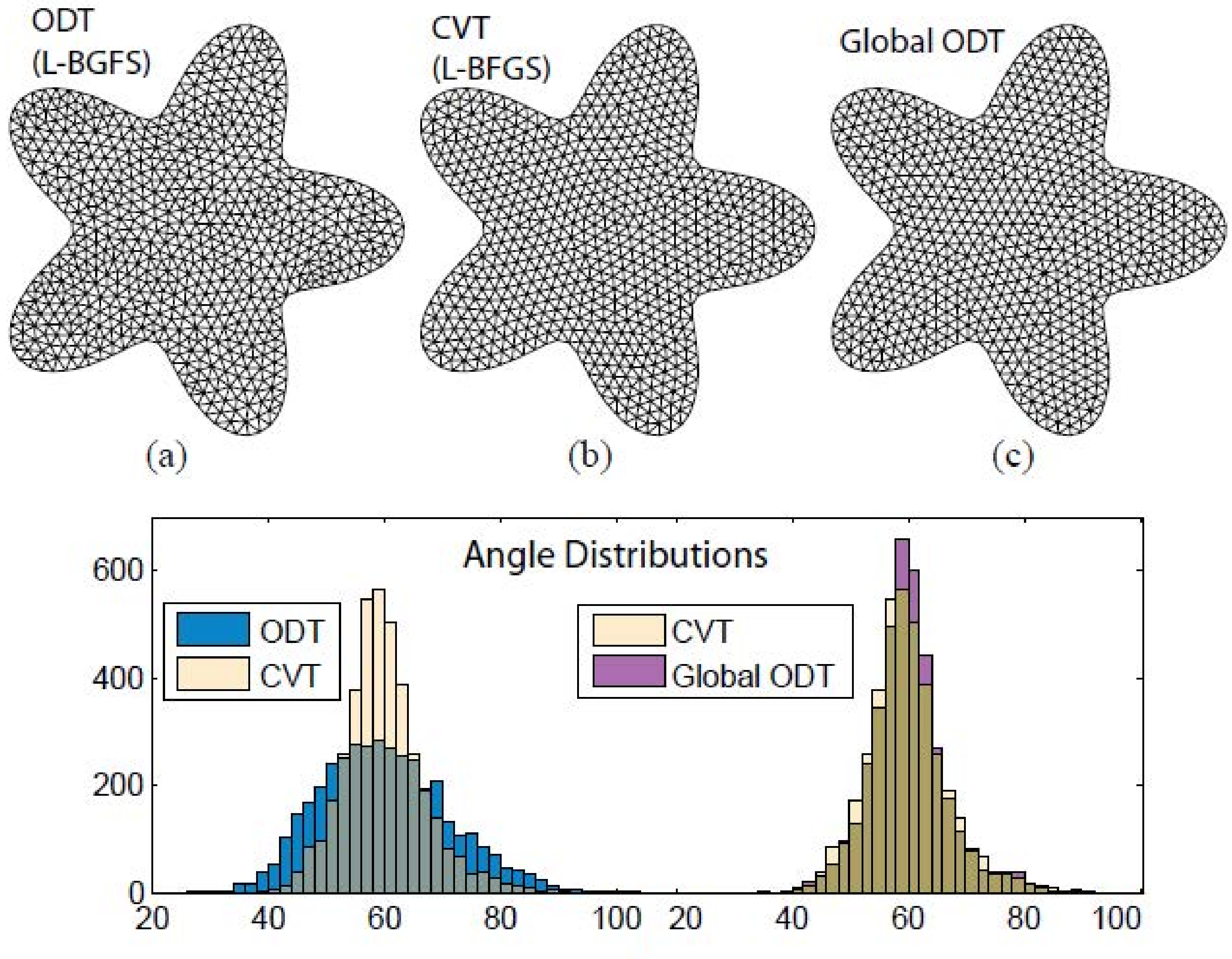
ODT
(L-BGFS)
CVT
(L-BFGS)
Global ODT
(a)
(b)
(c)
Angle Distributions
ODT
CVT
CVT
Global ODT
600
400
200
0
20
40
60
80
100
20
40
60
80
100

(d)

CVT vs. ODT (2)

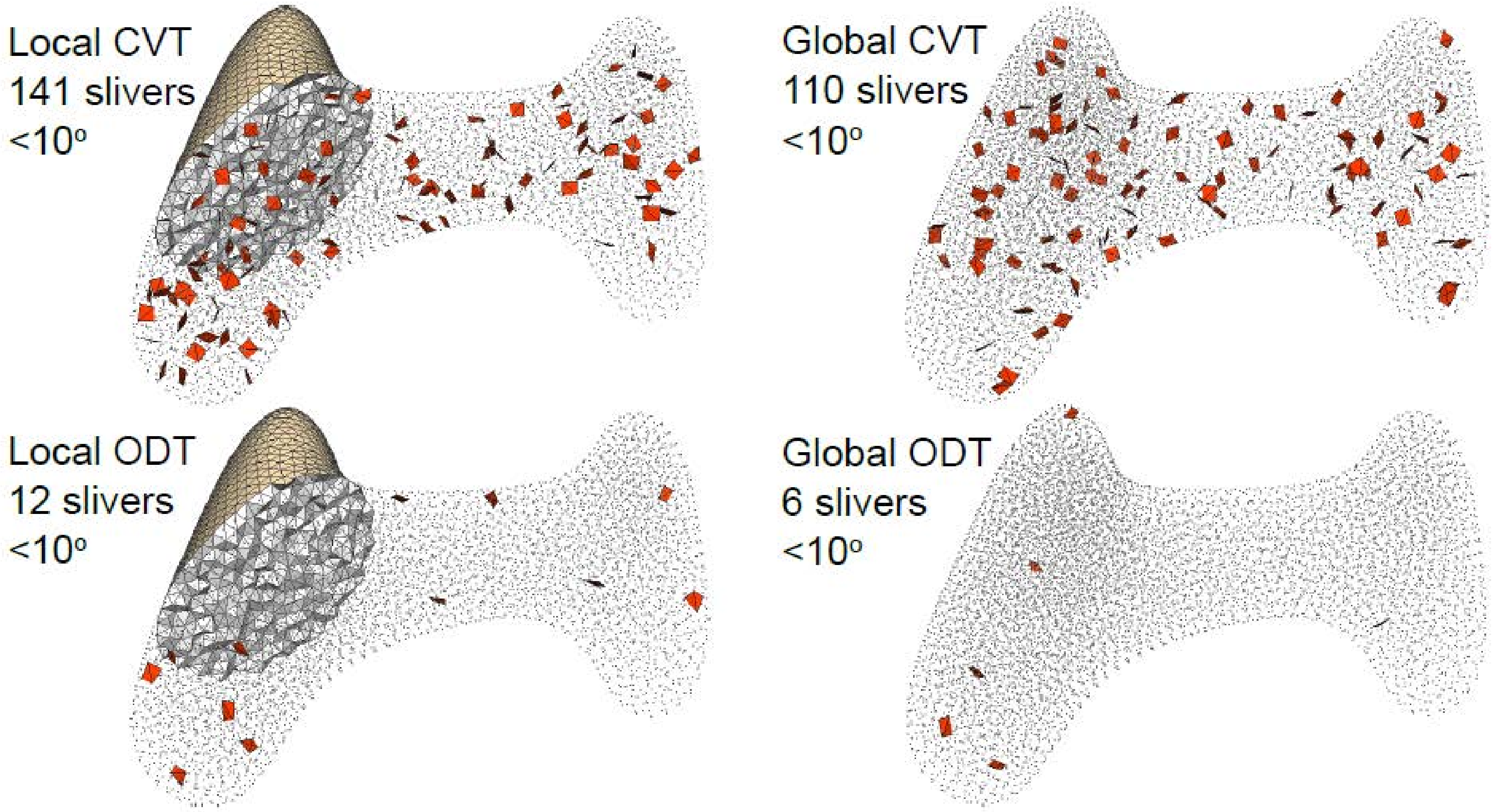
Local CVT
141 slivers
<10°
Global CVT
110 slivers
<10°
Local ODT
12 slivers
<10°
Global ODT
6 slivers
<10°

Constrained Centroidal Delaunay Mesh (CCDM)*

- For a compact surface $S \subset \mathbb{R}^3$, the CCDM energy function is defined as:

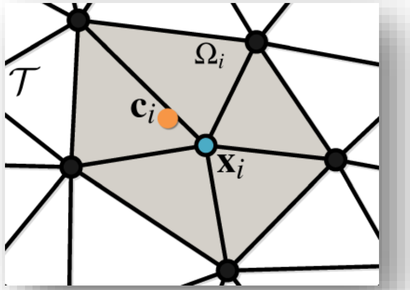

$$\mathcal{F}(\mathbf{X}, \mathcal{M}) = \sum_{i=1}^{n} \int_{\Omega_i} \rho(\mathbf{x}) \| \mathbf{x} - \mathbf{x}_i \|^2 \, \mathrm{d}\sigma$$

subject to: the vertices **X** lie on the surface *S*;
$\mathcal{M}$ is a Delaunay mesh of **X**;
Ω_i is 1-ring neighbor patch of $\mathbf{x}_i$.

Zhonggui Chen**, Juan Cao, Wenping Wang, *Isotropic Surface Remeshing Using Constrained Centroidal Delaunay Mesh*. ***Computer Graphics Forum (Proc. Pacific Graphics), 31(7): 2077–2085, 2012

CCDM Computation

- Optimization by a two-step iterative algorithm:
  - (*connectivity update*) generate the Delaunay mesh $\mathcal{M}$
  - (*vertex relocation*) move each vertex $\mathbf{x}_i$ to the centroid $\mathbf{c}_i$ of the corresponding patch Ω_i

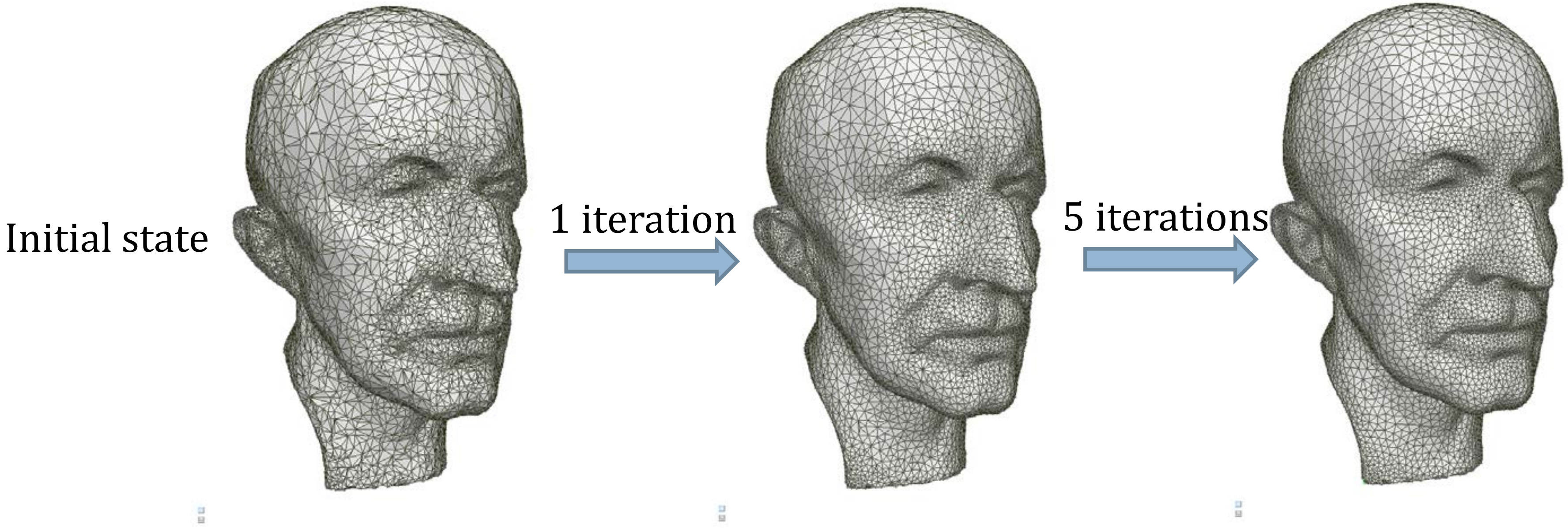

CCDM Result

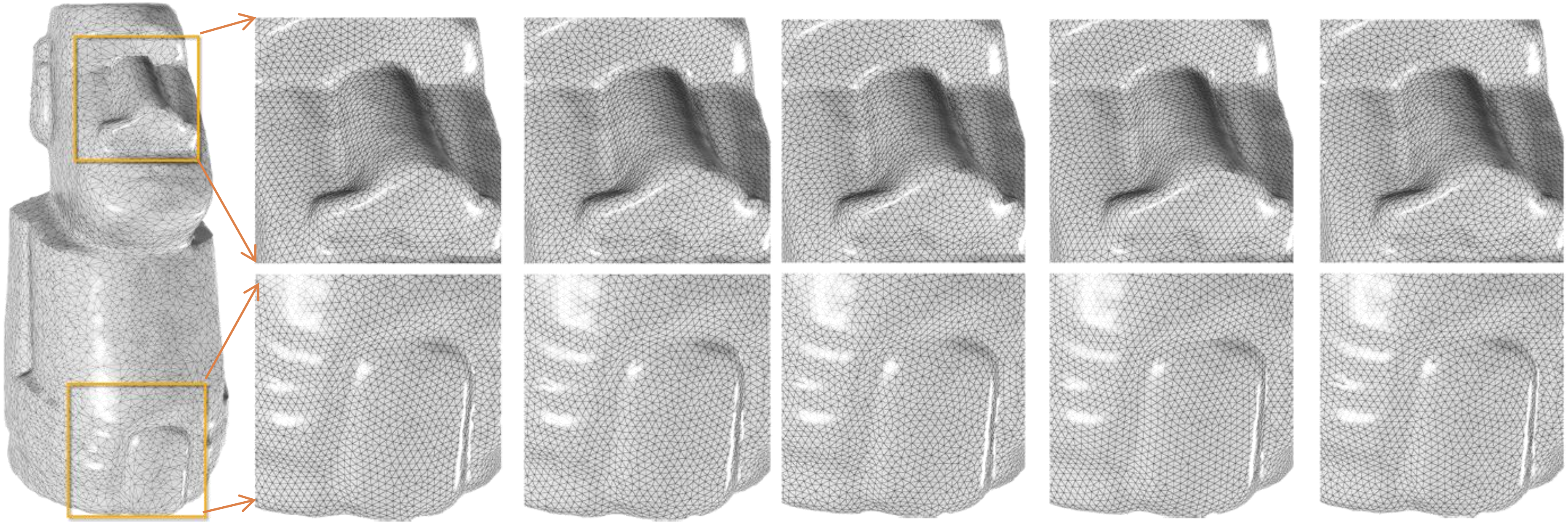

Input | Ours | [Botsch and Kobbelt 04] | [Valette et al. 08] | [Yan et al. 09] | [Fuhrmann et a. 10]

Model (#vert)	Method	Time (sec)	∠ (deg) Avg	∠ (deg) Min	$< 30^o$ (%)	Aspect Ratio Avg	Aspect Ratio Min	Error (10^{-3})
Moai (10,002 – 30,000)	Ours	21.35	54.21	38.22	0	0.934	0.645	3.72
	[BK04]	4.12	51.93	33.16	0	0.907	0.632	3.21
	[VCP08]	15.99	50.98	31.51	0	0.886	0.538	2.94
CVT method	[YLL*09]	263.16	54.80	38.79	0	0.939	0.636	2.80
	[FAKG10]	157.09	53.62	38.02	0	0.922	0.638	3.21

III

Capacity-constrained Centroidal Voronoi Tessellation (CapCVT)

Zhonggui Chen, Zhan Yuan, Yi-King Choi, Ligang Liu, Wenping Wang. **Variational Blue Noise Sampling**. *IEEE Transactions on Visualization and Computer Graphics*,18(10):1784-1796,2012

Capacity-Constrained Voronoi Tessellation (CapVT)

A Voronoi tessellation $\{V_i\}_{i=1}^{n}$ is called a *capacity-constrained Voronoi tessellation* (CapVT) if its Voronoi cells satisfy the constraints:

$$\int_{V_i} \varrho(\mathbf{x}) \, \mathrm{d}\sigma = k_i \ (i = 1, \ldots, n),$$

where $\varrho(\mathbf{x}) \geq 0$ is a density function defined in Ω and the k_i are capacity constraints with $k_i > 0$ and $\sum_{i=1}^{n} k_i = \int_{\Omega} \varrho(\mathbf{x}) \, \mathrm{d}\sigma$.

CapVT – Application

- Voronoi Treemap: visualization of attributed hierarchical data

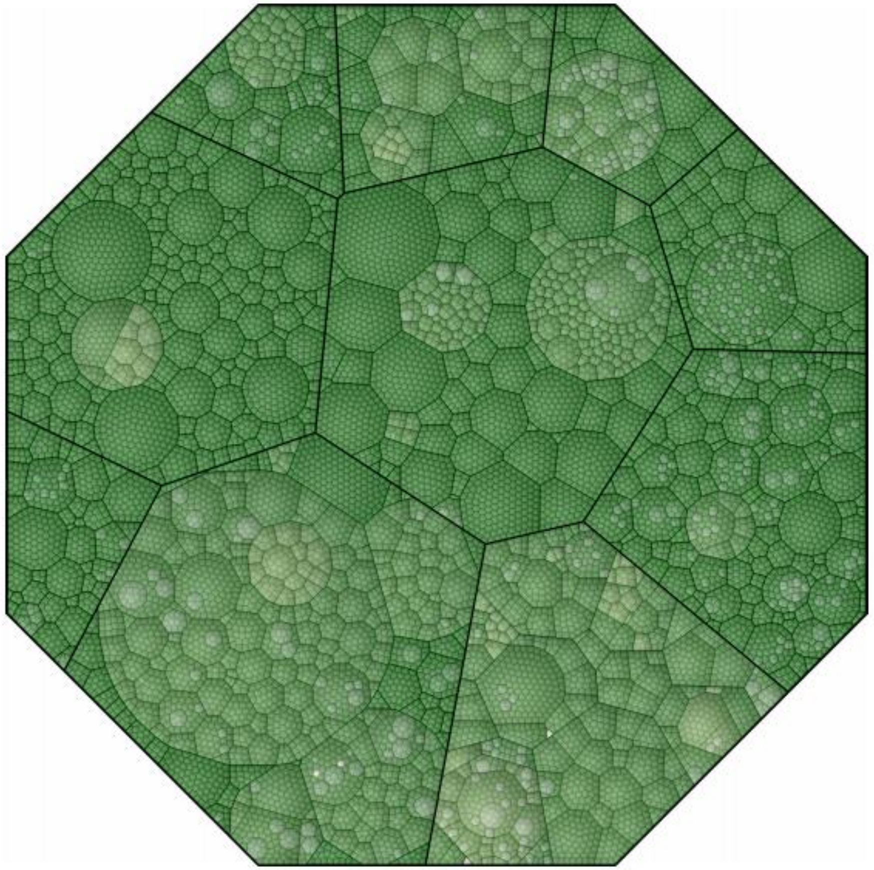

CapVT: Energy Function

- CapVT energy function:

$$E_{\mathrm{CapVT}}(\mathbf{X}) = \sum_{i=1}^{n} \left(\int_{V_i} \varrho(\mathbf{x}) \, \mathrm{d}\sigma - k_i \right)^2 .$$

- Assume each Voronoi cell has the same capacity, that is $k_i = k$ for all i. We can define the CapVT energy function as

$$E_{\mathrm{CapVT}}(\mathbf{X}) = \sum_{i=1}^{n} \left(\int_{V_i} \varrho(\mathbf{x}) \, \mathrm{d}\sigma \right)^2$$

Optimization by L-BFGS

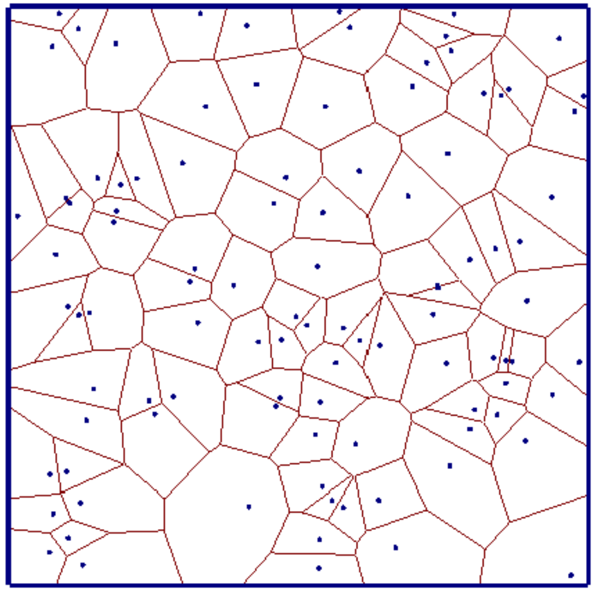

Initial state

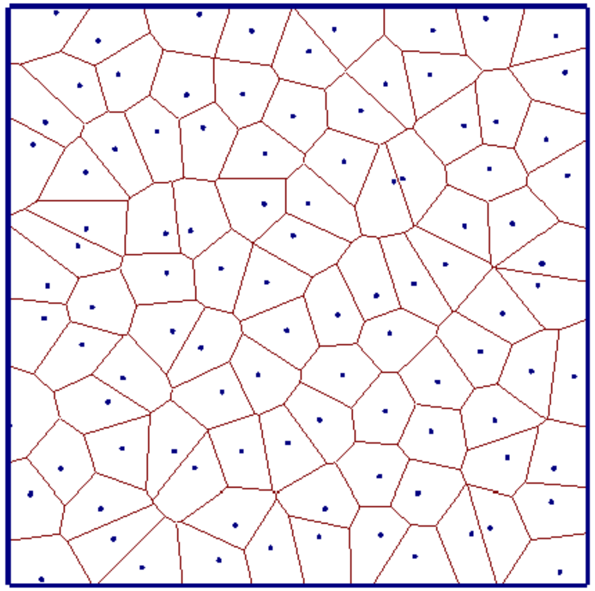

CapVT by L-BFGS

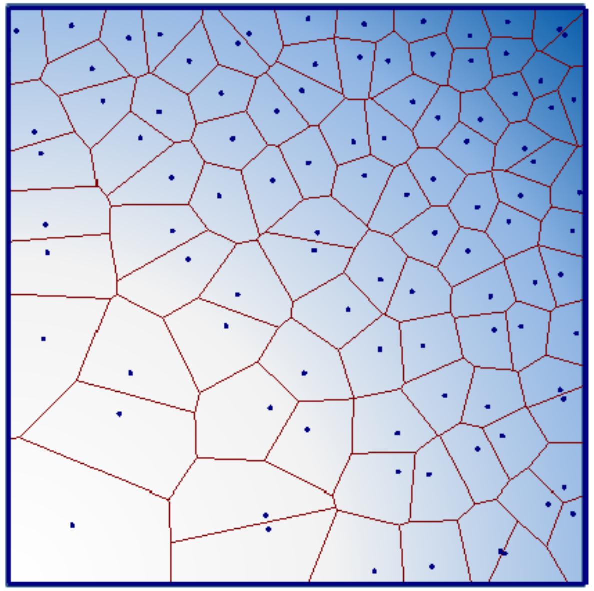

CapVT with density

Capacity-constrained Centroidal Voronoi Tessellation (CapCVT)

- CapCVT energy function:

$$
\begin{aligned}
E_{\text{CapCVT}}(\mathbf{X}) =& E_{\text{CVT}}(\mathbf{X}) + \lambda E_{\text{CapVT}}(\mathbf{X}) \\
=& \sum_{i=1}^{n} \int_{V_i} \rho(\mathbf{x}) \|\mathbf{x} - \mathbf{x}_i\|^2 \mathrm{d}\sigma + \lambda \sum_{i=1}^{n} \left(\int_{V_i} \varrho(\mathbf{x}) \mathrm{d}\sigma \right)^2
\end{aligned}
$$

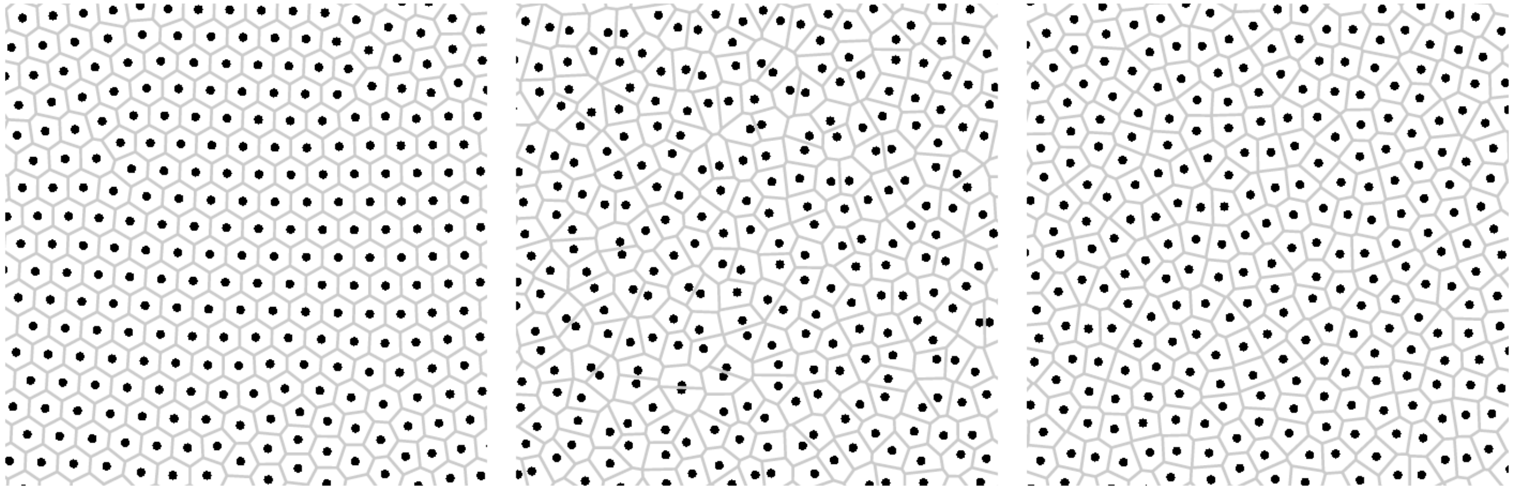

(a) CVT (b) CapVT (c) CapCVT

Blue Noise Distribution

- (Left) A uniformly distributed yet randomly located point set
- (Right) The typical power spectrum, radially averaged power spectrum and anisotropy of blue noise distributions.

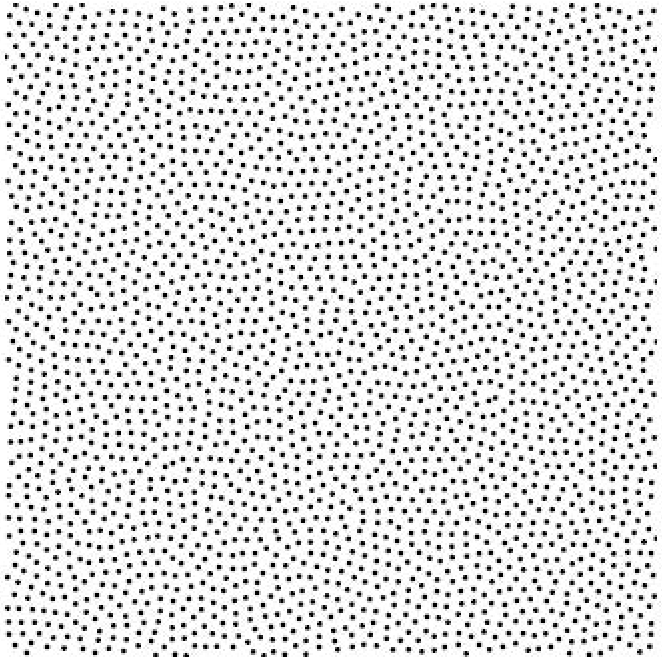

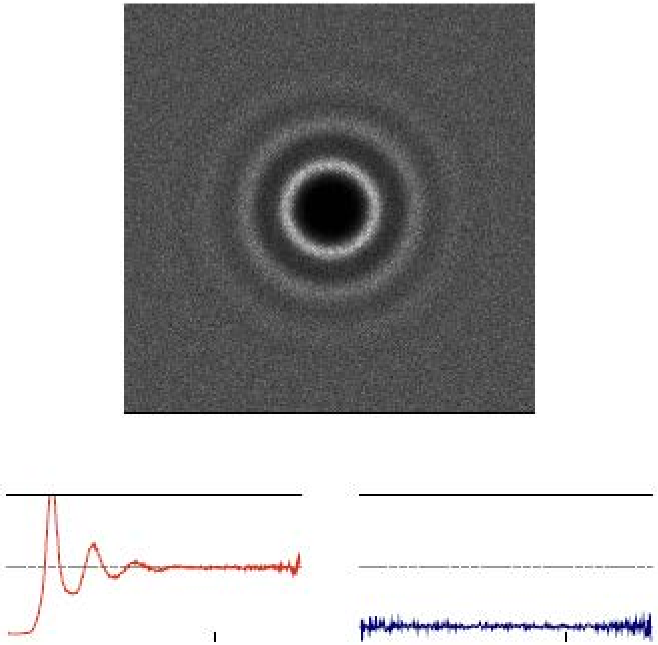

Sampling by CVT Method

- CVT method develops "regularity artifacts" in resulting point distributions

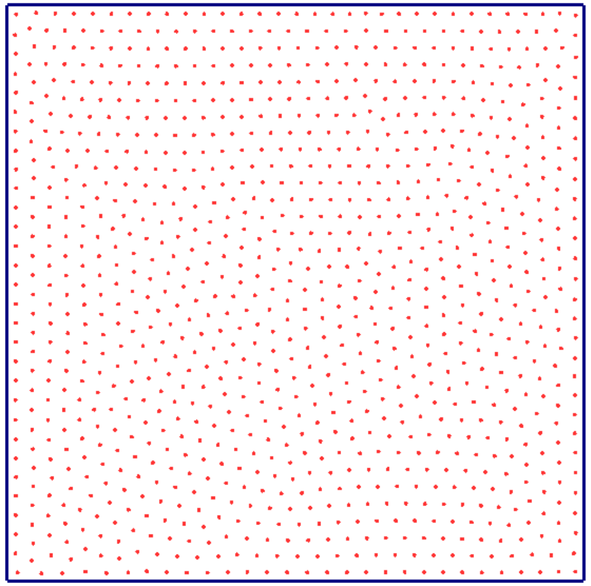

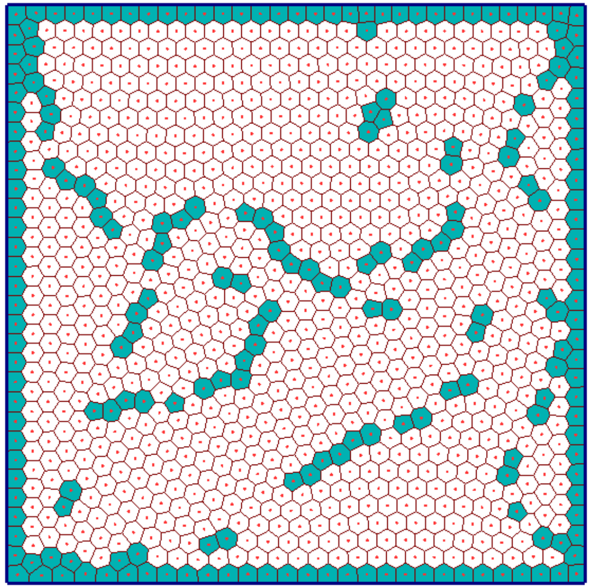

Left: point distribution obtained by CVT method
Right: Voronoi tessellation with non-hexagonal cells marked

Sampling by CVT Method

- Spectral characteristics of the point distributions obtained by CVT

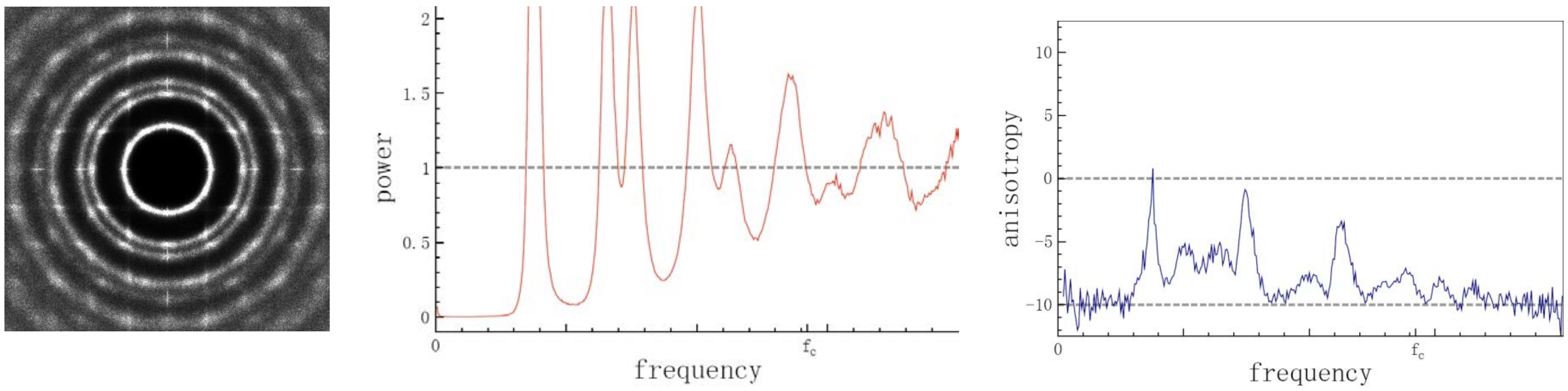

Left: power spectrum; middle: radially averaged power spectrum;
right: anisotropy.

CapCVT Sampling on Image

(left) Input image as a density map; (right) sampling result by our method.

CapCVT Sampling on Surface

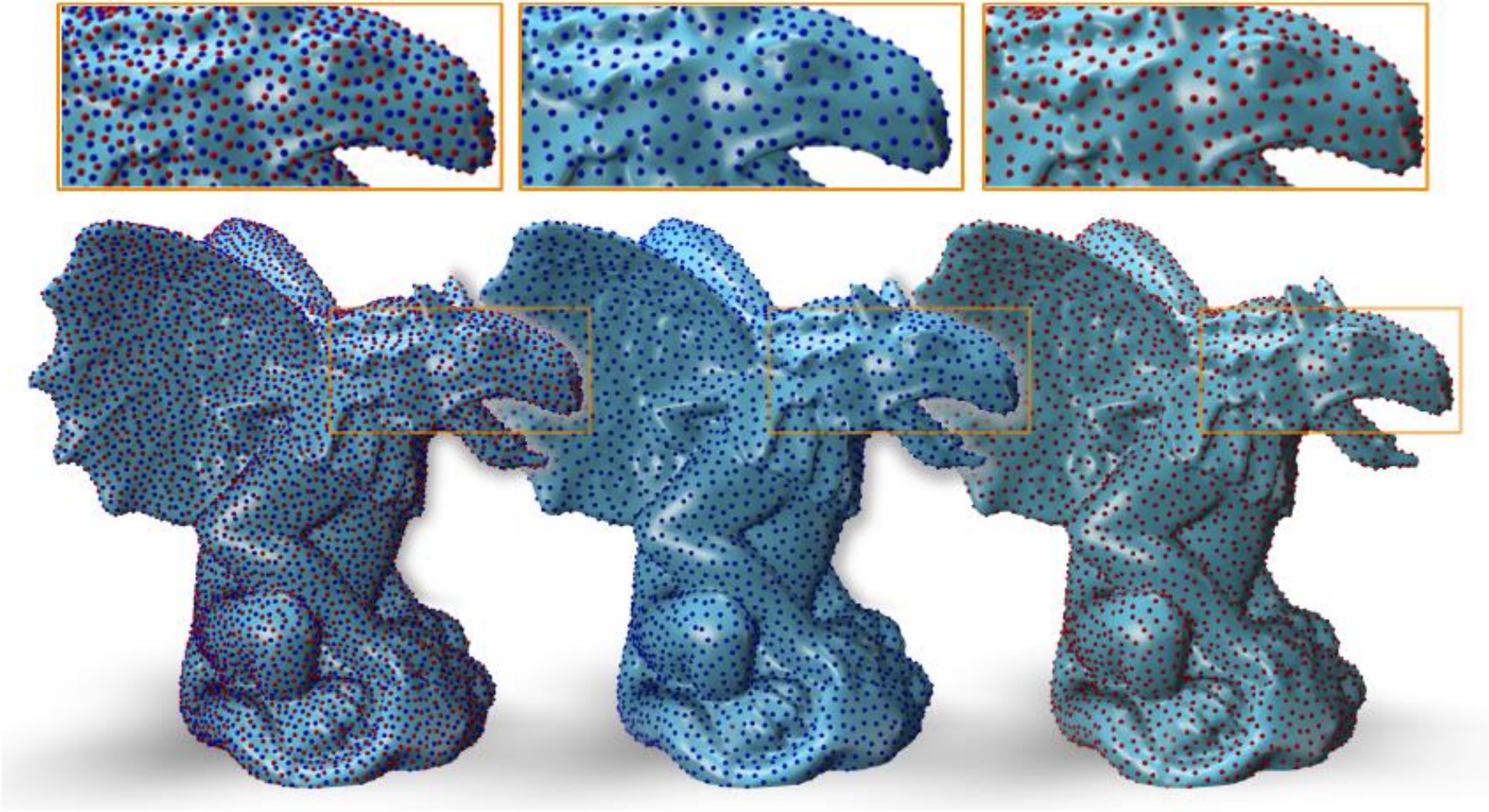

IV Capacity Constrained Centroidal Power Diagram (CPD)

Shiqin Xin, Bruno Levy, Zhonggui Chen, Chu Lei, Yaohui Yu, Changhe Tu, Wenping Wang. **Centroidal power diagrams with capacity constraints – computation, applications and extension**. *ACM Transactions on Graphics*, 35, 6, Article 244:1-12, 2016

Capacity Constrained Centroidal Power Diagram (CPD)*

- Problem Formulation
  - To find the ***power diagram*** with the sites **X** and the weights W such that the total cost

$$\mathcal{E}(\mathbf{X}, W) = \sum_i \int_{\mathcal{V}_i^w} \rho(\mathbf{x}) \left\|\mathbf{x} - \mathbf{x}_i\right\|^2 d\mathbf{x}$$

is minimized, subject to the constraints

$$m_i = \int_{\mathcal{V}_i} \rho(\mathbf{x}) \, d\mathbf{x} \equiv m.$$

Capacity Constrained Centroidal Power Diagram (CPD)*

- Problem Formulation
  - It is equivalent to finding a saddle point of the following functional:

$$\mathcal{F}(\mathbf{X}, W) = \mathcal{E}(\mathbf{X}, W) - \sum_i w_i \left(m_i - m\right)$$

where

$$\mathcal{E}(\mathbf{X}, W) = \sum_i \int_{\mathcal{V}_i^w} \rho(\mathbf{x}) \left\|\mathbf{x} - \mathbf{x}_i\right\|^2 d\mathbf{x}$$

and

$$m_i = \int_{\mathcal{V}_i^w} \rho(\mathbf{x}) \; d\mathbf{x}.$$

Computing CPD using L-BFGS

Input: domain $\mathcal{D}$, density ρ, cost kernel d, number of points n, capacity constraints $\{c_i\}$ and a threshold ϵ as the termination condition.

Initialization: set $k = 0$ and X_0 to n randomly generated sites.

repeat *//L-BFGS*

  repeat *//To meet the capacity constraints*

    Update W_k by Newton's method

  until $||\nabla_W F(X, W)|| < 10^{-12}$

  Compute the gradients $\nabla_X F(X, W^*(X)$ in Eqn. (10)

  Compute ΔX using the L-BFGS updating rule

  $X_{k+1} \leftarrow X_k$

  $k \leftarrow k + 1$

until $||\nabla_X F(X, W^*(X))|| < \epsilon$

repeat *//To meet the capacity constraints*

  Update W_k by Newton's method

until $||\nabla_W F(X, W)|| < 10^{-12}$

Output: (X_k, W_k)

Algorithm 1: Computing CPD using L-BFGS.

CPD with General Cost Kernels

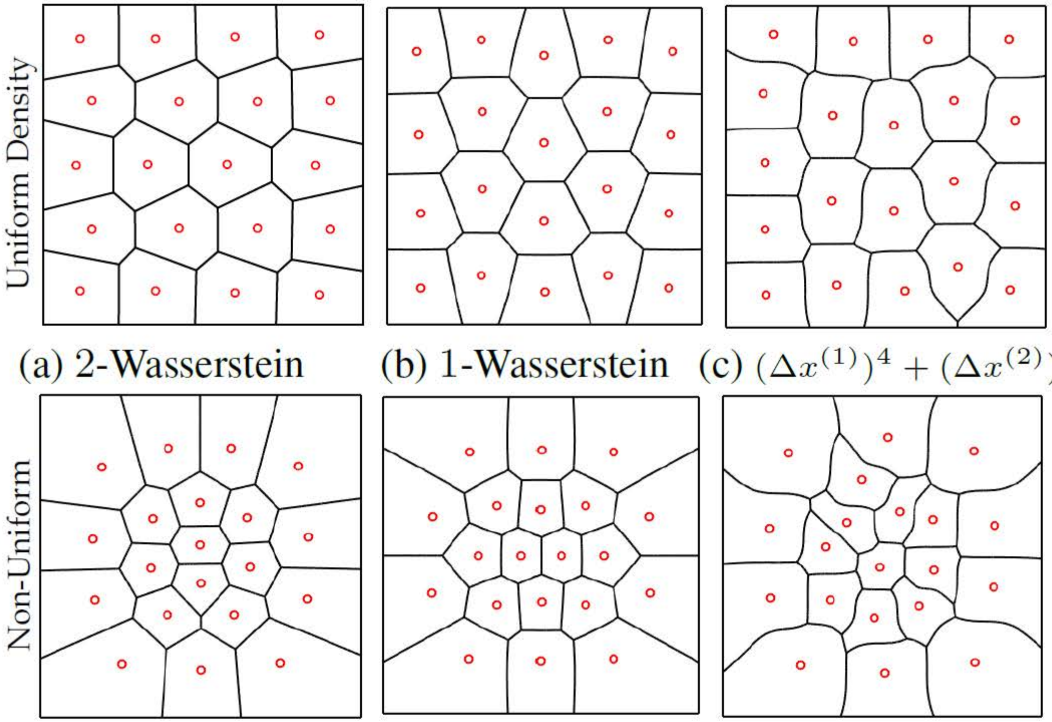

(a) 2-Wasserstein (b) 1-Wasserstein (c) $(\Delta x^{(1)})^4 + (\Delta x^{(2)})^4$

(d) 2-Wasserstein (e) 1-Wasserstein (f) $(\Delta x^{(1)})^4 + (\Delta x^{(2)})^4$

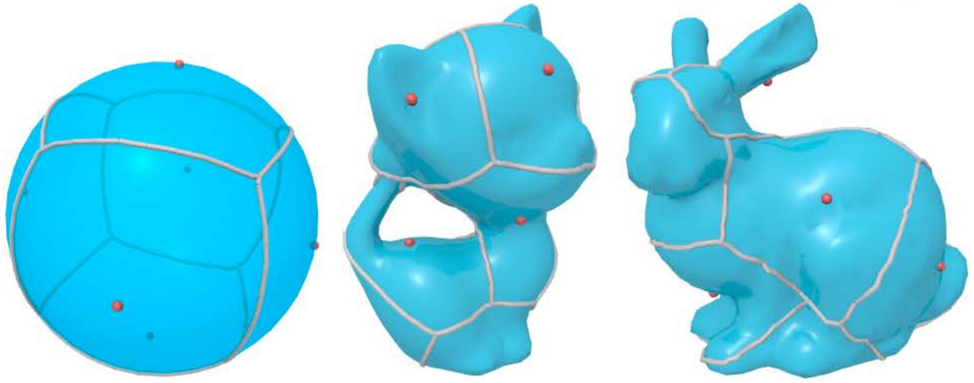

(g) Geodesic distance (h) Squared (i) Cubic

Figure 3: *Our algorithm can be extended to general cost kernels.*

V

Optimal Voronoi Tessellation (OVT)

Budninskiy M, Liu B, De Goes F, et al. **Optimal Voronoi tessellations with Hessian-based anisotropy**. ACM Transactions on Graphics, 35(6): 242, 2016.

Centroidal Voronoi Tessellation

- *Definition* (Variational point of view)
  - CVT energy function:

$$\mathcal{E}_{CVT}(\mathbf{X},\mathcal{V}) = \sum_{i=1}^{n}\int_{V_i}\left\|\mathbf{x}-\mathbf{x}_i\right\|^2 d\mathbf{x} = \sum_{i=1}^{n}\int_{V_i}\left(\mathbf{x}^2 - \left(2\mathbf{x}_i^T\mathbf{x}-\mathbf{x}_i^2\right)\right)d\mathbf{x}$$

- Geometric interpretation

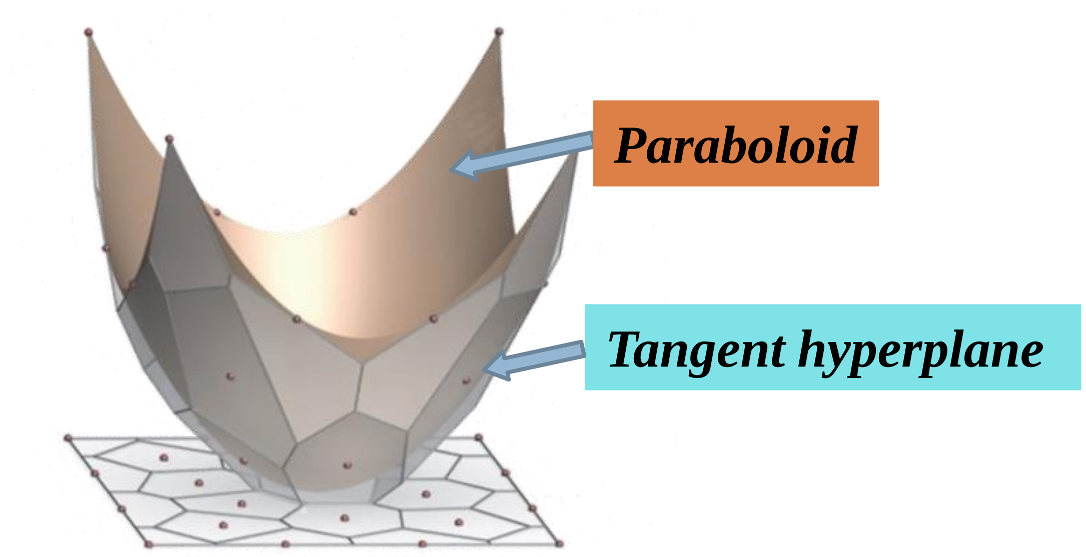

Optimal Voronoi Tessellation (OVT)

[Budninskiy et.al., ACM TOG 2016]

- OVT energy function:

$$\mathcal{E}_{OVT}(\mathbf{X},\mathcal{V}) = \| f - f_T \|_{L^1} = \sum_{i=1}^{n} \int_{V_i} \left(f(\mathbf{x}) - T_i(\mathbf{x}) \right) \mathrm{d}\mathbf{x},$$

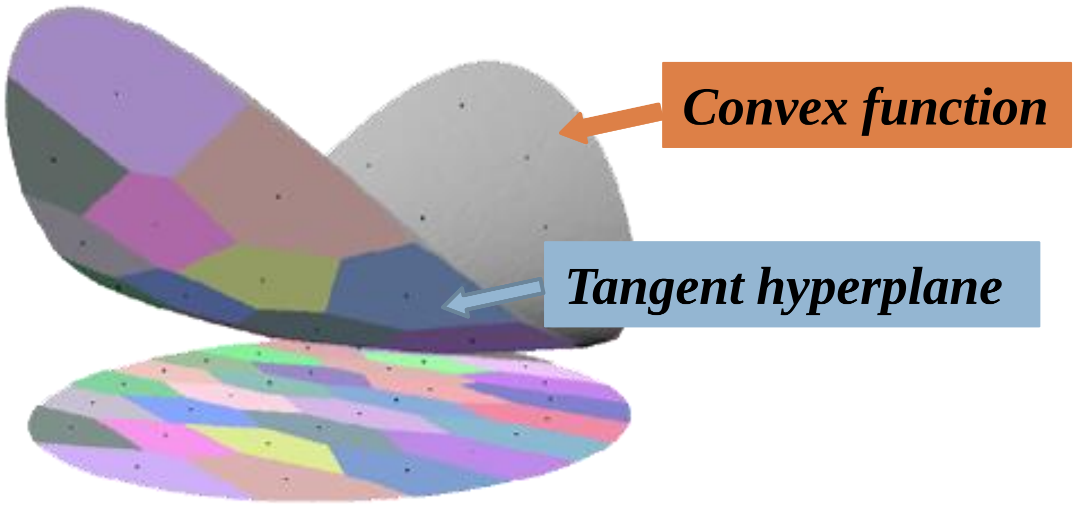

$$T_i(\mathbf{x}) = \nabla f(\mathbf{x}_i) \cdot (\mathbf{x} - \mathbf{x}_i) + f(\mathbf{x}_i)$$

Optimal Voronoi Tessellations

- [Budninskiy et.al., ACM TOG 2016]

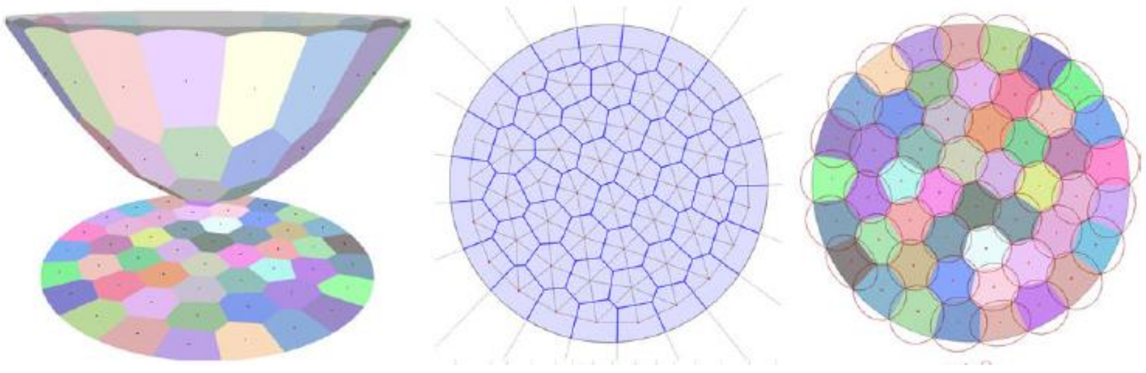

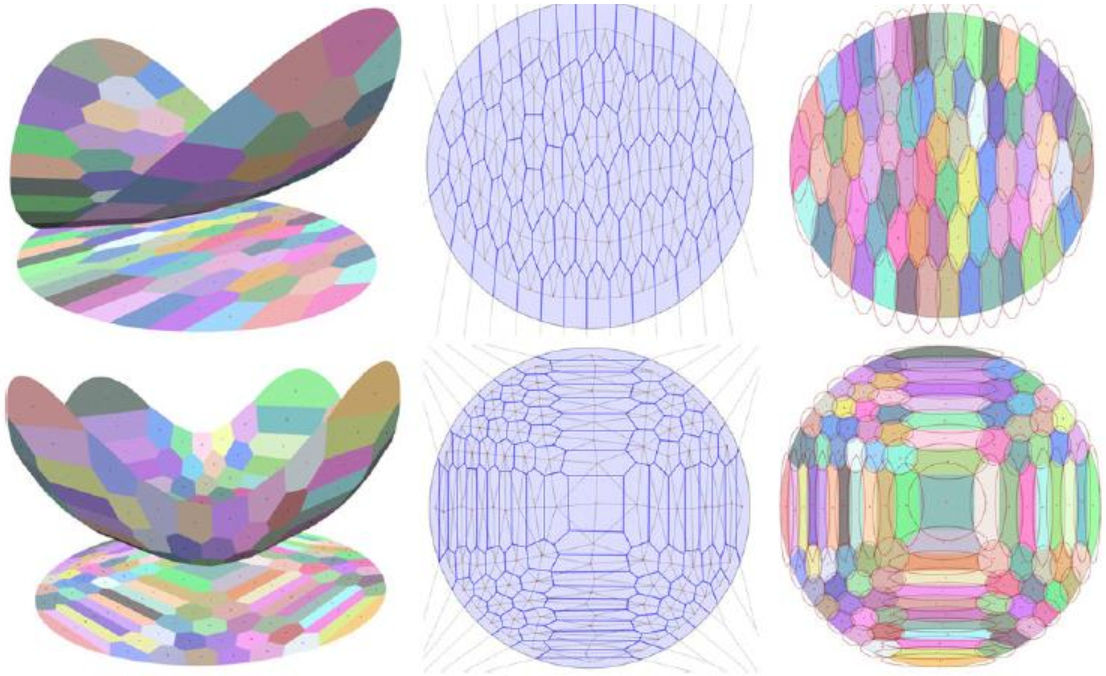

VI Optimal Power Diagram (OPD)

*Yanyang Xiao, Zhonggui Chen, Juan Cao, Yongjie Jessica Zhang, Cheng Wang. **Optimal Power Diagrams via Function Approximation**. *Computer-Aided Design* (Proc. SPM; Best Paper Award 1st Place), 102:52-60, 2018

Optimal Power Diagram (OPD)*

- Energy function formulation:

OVT function $\mathcal{E}_{OVT}(\mathbf{X},\mathcal{V}) = \| f - f_T \|_{L^1} = \sum_{i=1}^{n} \int_{V_i} (f(\mathbf{x}) - T_i(\mathbf{x}))\mathrm{d}\mathbf{x},$

Convex function: $f(\mathbf{x})$

Tangent hyperplane: $T_i(\mathbf{x})$

Optimal Power Diagram (OPD)

- Energy function formulation:

OVT function $$\mathcal{E}_{OVT}(\mathbf{X}, \mathcal{V}) = \| f - f_T \|_{L^1} = \sum_{i=1}^{n} \int_{V_i} \left(f(\mathbf{x}) - T_i(\mathbf{x}) \right) \mathrm{d}\mathbf{x},$$

Convex function ($f(\mathbf{x})$) — Tangent hyperplane ($T_i(\mathbf{x})$)

Ours $$\mathcal{E}(\mathcal{V}, \{P_i(\mathbf{x})\}_{i=1}^{n}) = \| f - f_P \|_{L^1} = \sum_{i=1}^{n} \int_{V_i} \left| f(\mathbf{x}) - P_i(\mathbf{x}) \right| \mathrm{d}\mathbf{x},$$

Non-convex function ($f(\mathbf{x})$) — Best fitting hyperplane ($P_i(\mathbf{x})$)

Optimal Power Diagram (OPD)

- Energy function formulation:

OVT function $\mathcal{E}_{OVT}(\mathbf{X},\mathcal{V}) = \| f - f_T \|_{L^1} = \sum_{i=1}^{n} \int_{V_i} (f(\mathbf{x}) - T_i(\mathbf{x}))\mathrm{d}\mathbf{x},$

Convex function — $f(\mathbf{x})$; Tangent hyperplane — $T_i(\mathbf{x})$

Ours $\mathcal{E}(\mathcal{V},\{P_i(\mathbf{x})\}_{i=1}^{n}) = \| f - f_P \|_{L^1} = \sum_{i=1}^{n} \int_{V_i} |f(\mathbf{x}) - P_i(\mathbf{x})|\mathrm{d}\mathbf{x},$

Non-convex function — $f(\mathbf{x})$; Best fitting hyperplane — $P_i(\mathbf{x})$

$$\mathcal{E}(\mathcal{V},\{P_i(\mathbf{x})\}_{i=1}^{n}) = \| f - f_P \|_{L^2}^2 = \sum_{i=1}^{n} \int_{V_i} (f(\mathbf{x}) - P_i(\mathbf{x}))^2 \mathrm{d}\mathbf{x}$$

Optimal Power Diagram (OPD)

- Energy function formulation

$$\mathcal{E}(\mathcal{V},\{P_i(\mathbf{x})\}_{i=1}^{n}) = \| f - f_P \|_{L^2}^2 = \sum_{i=1}^{n}\int_{V_i}\left(f(\mathbf{x}) - P_i(\mathbf{x})\right)^2 \mathrm{d}\mathbf{x},$$

① Restrict $\mathcal{V}$ to power diagram, determined by $(\mathbf{X}, W) = \left(\{\mathbf{x}_i\}_{i=1}^{n}, \{w_i\}_{i=1}^{n}\right)$

② When $\mathcal{V}$ is fixed, best-fit hyperplane on each cell is determined, denoted by $P_i^*(\mathbf{x})$

$$\mathcal{E}_{OPD}(\mathbf{X}, W) = \| f - f_P \|_{L^2}^2 = \sum_{i=1}^{n}\int_{V_i}\left(f(\mathbf{x}) - P_i^*(\mathbf{x})\right)^2 \mathrm{d}\mathbf{x},$$

Optimal Power Diagram (OPD)

- OPD energy

$$\mathcal{E}_{OPD}(\mathbf{X},W) = \| f - f_P \|_{L^2}^2 = \sum_{i=1}^{n} \int_{V_i} \left(f(\mathbf{x}) - P_i^*(\mathbf{x}) \right)^2 \mathrm{d}\mathbf{x}$$

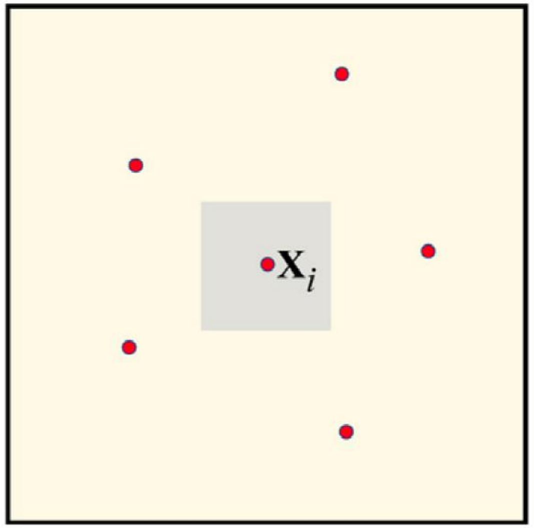

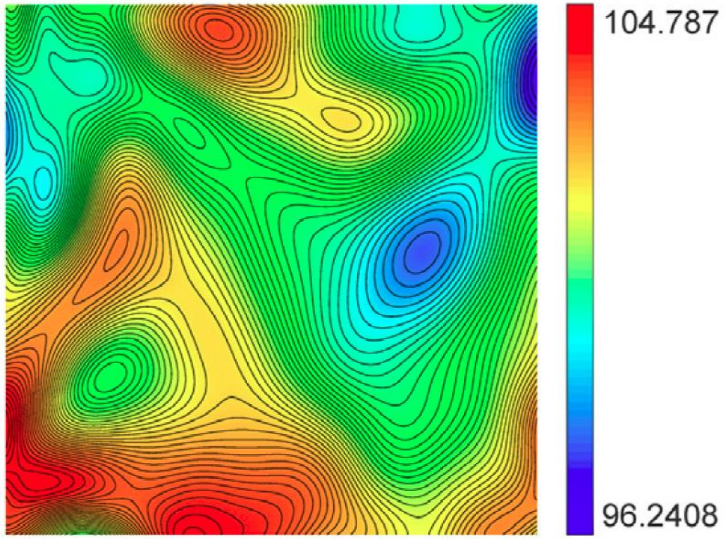

Energy landscape near $\mathbf{x}_i$ with $f(\mathbf{x}) = \sin(\pi(x+0.5))\cos(\pi y)$

Optimization Framework

- Observations

$$f\left(x,y\right)=100x^2+y^2,-1\le x,y\le 1$$

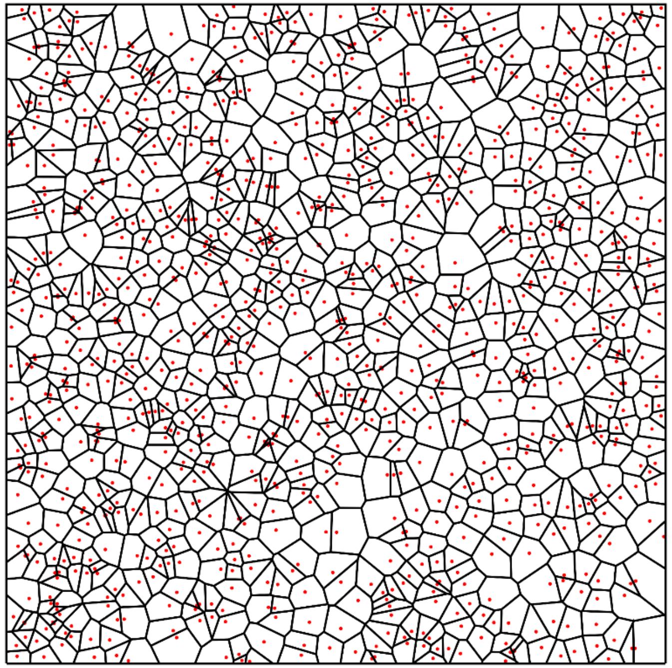

Random initialization

Optimization Framework

- Observations

$$f\left(x,y\right)=100x^2+y^2,-1\le x,y\le 1$$

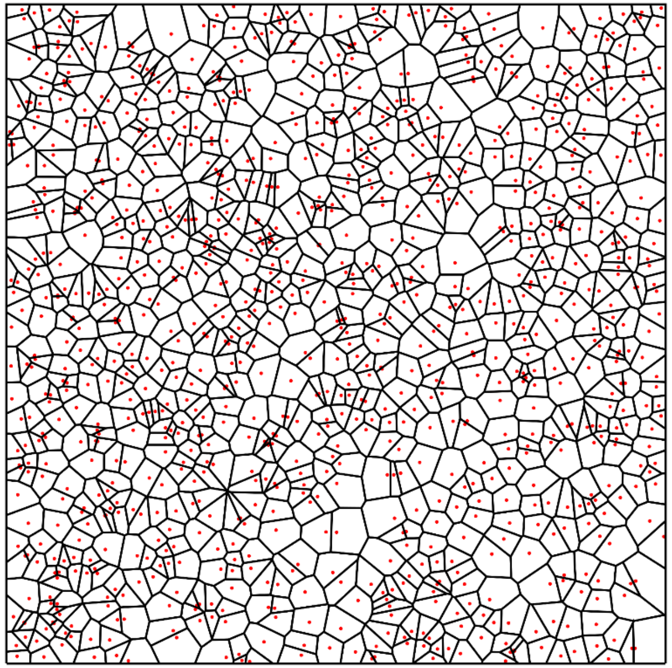

Random initialization

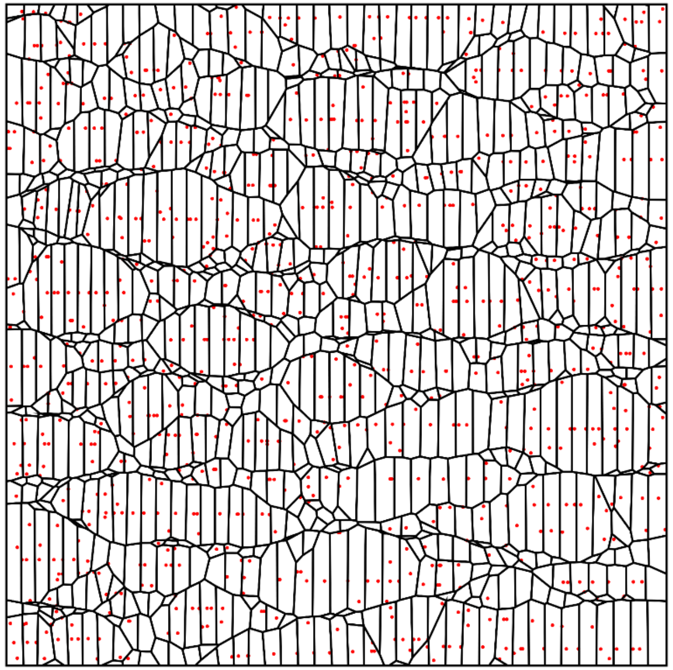

Optimizing $\left(\mathbf{X},W\right)$ simultaneously

Optimization Framework

- Observations

$$f(x, y) = 100x^2 + y^2, -1 \le x, y \le 1$$

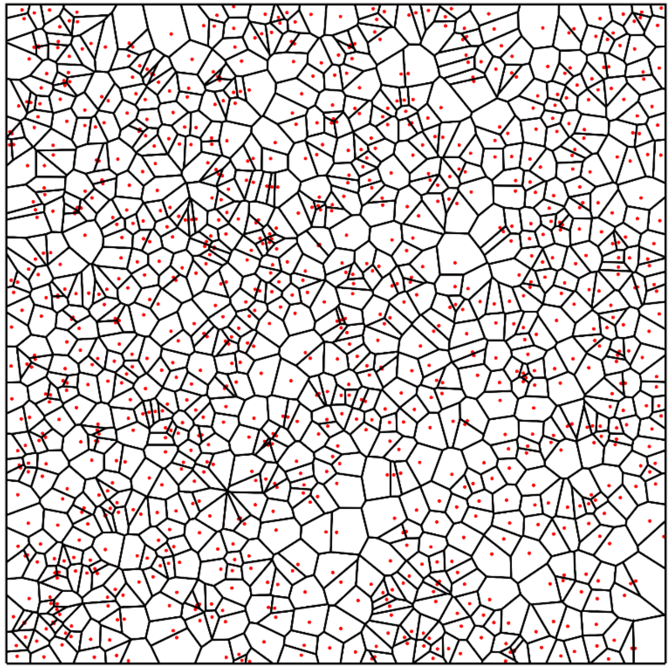

Random initialization

Optimization Framework

- Observations

$$f\left(x,y\right)=100x^2+y^2, -1\leq x,y\leq 1$$

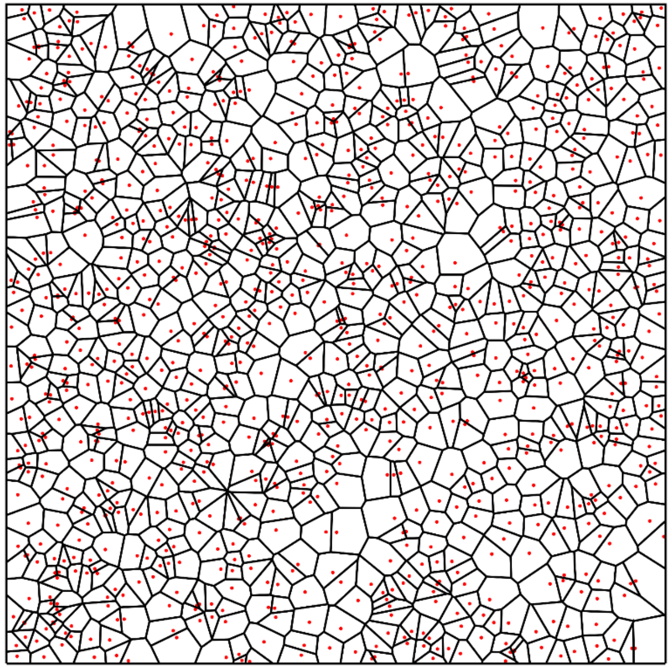

Random initialization

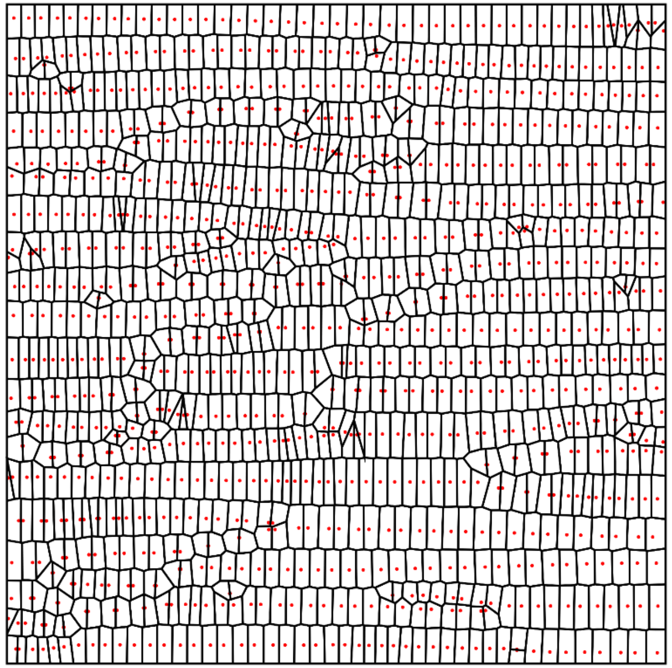

Position optimization only

Optimization Framework

- Observations

$$f\left(x,y\right)=100x^2+y^2,-1\le x,y\le 1$$

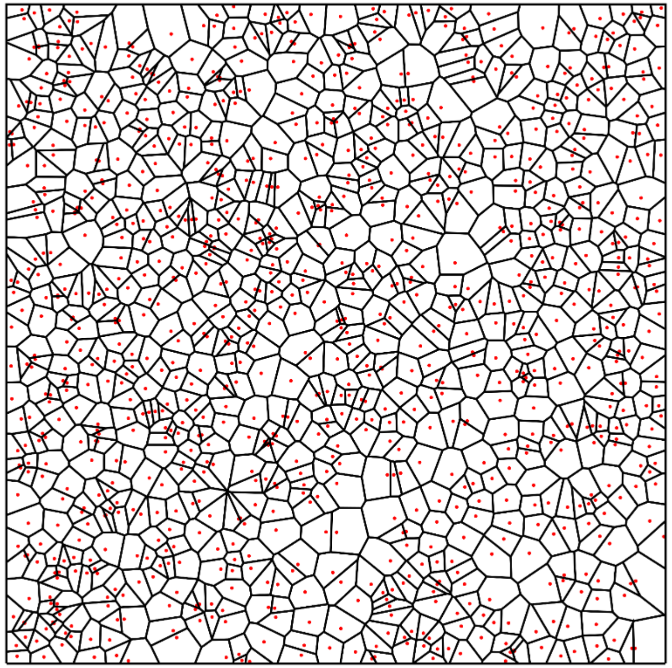

Random initialization

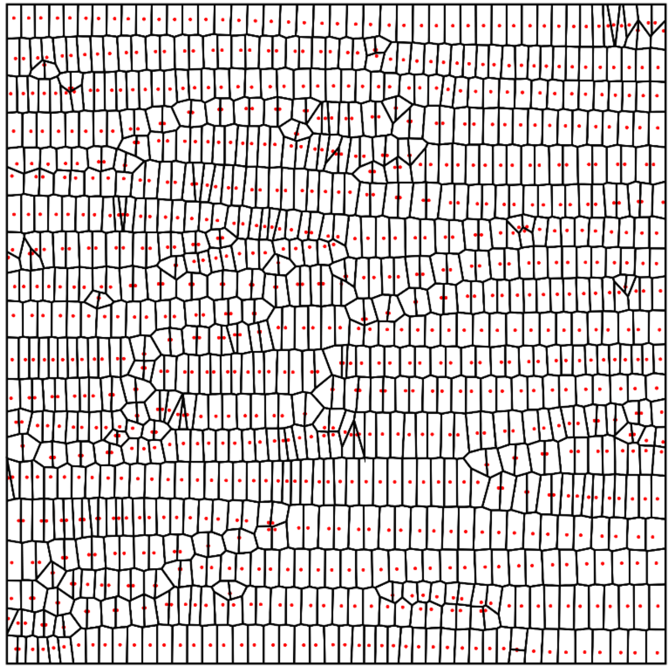

Position optimization only

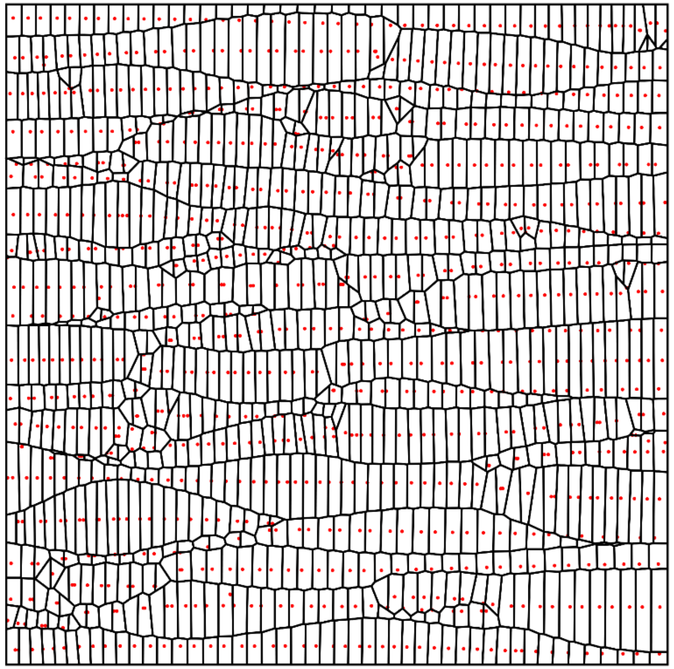

Position-weight optimization based on previous result

Optimization Framework

- Overview

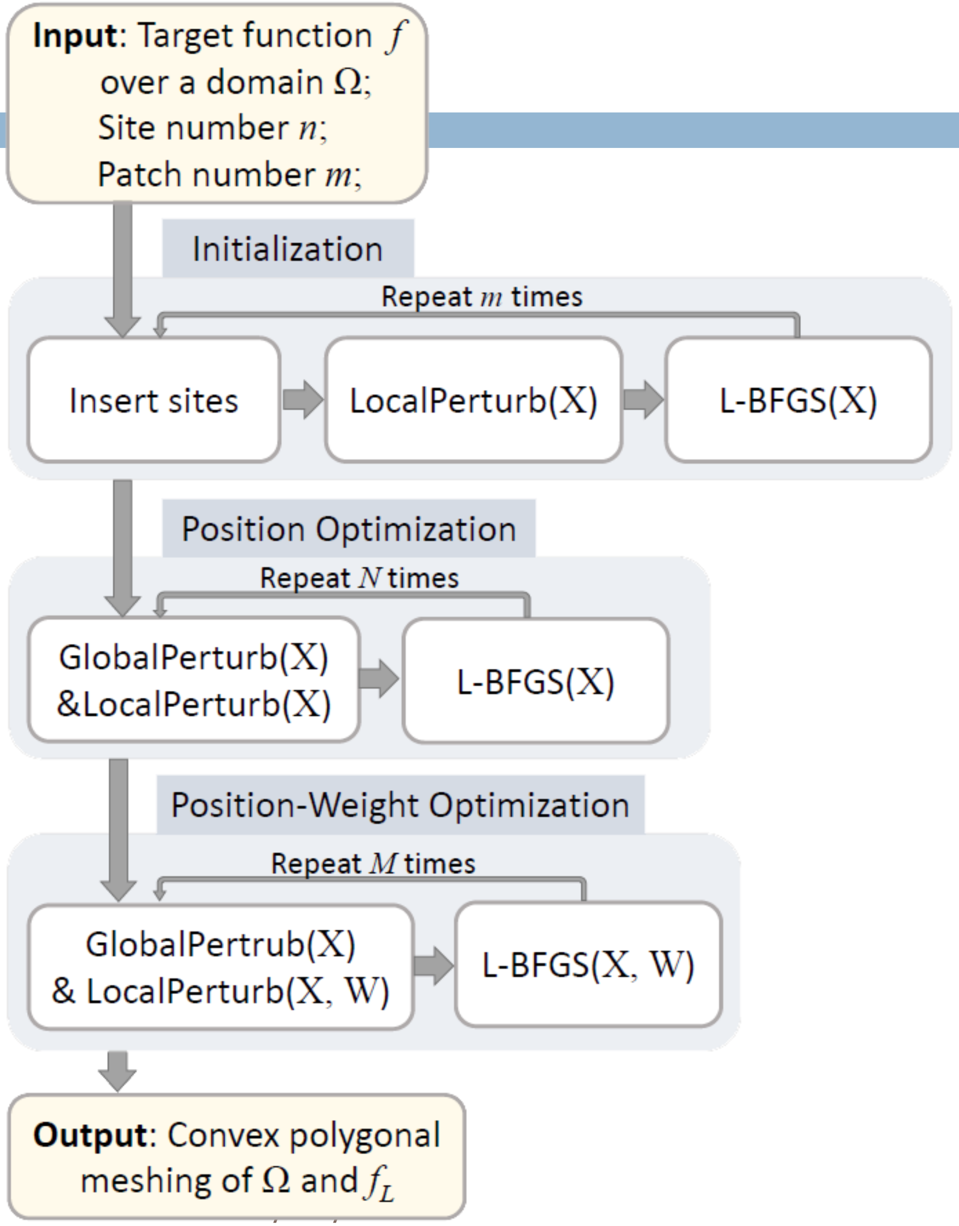

Optimization Framework

- Overview

(1) Initialization:

Insert and optimize site positions

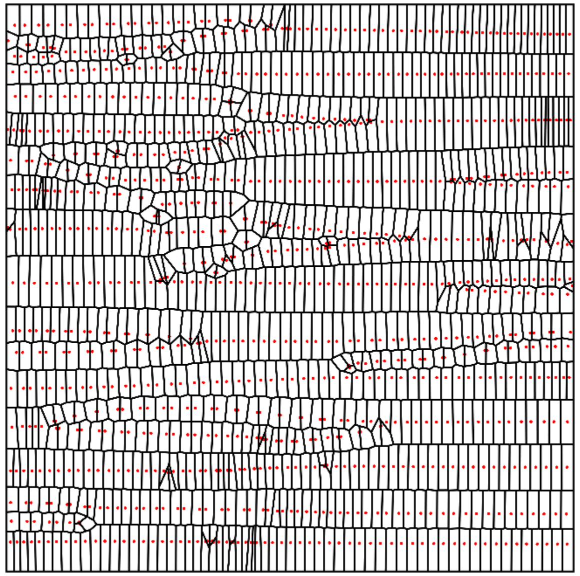

Random insertion

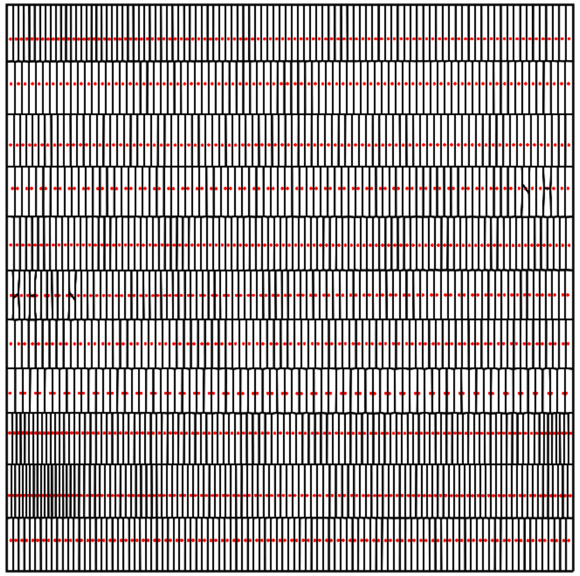

PCA-based insertion

$$f(x,y) = 100x^2 + y^2$$

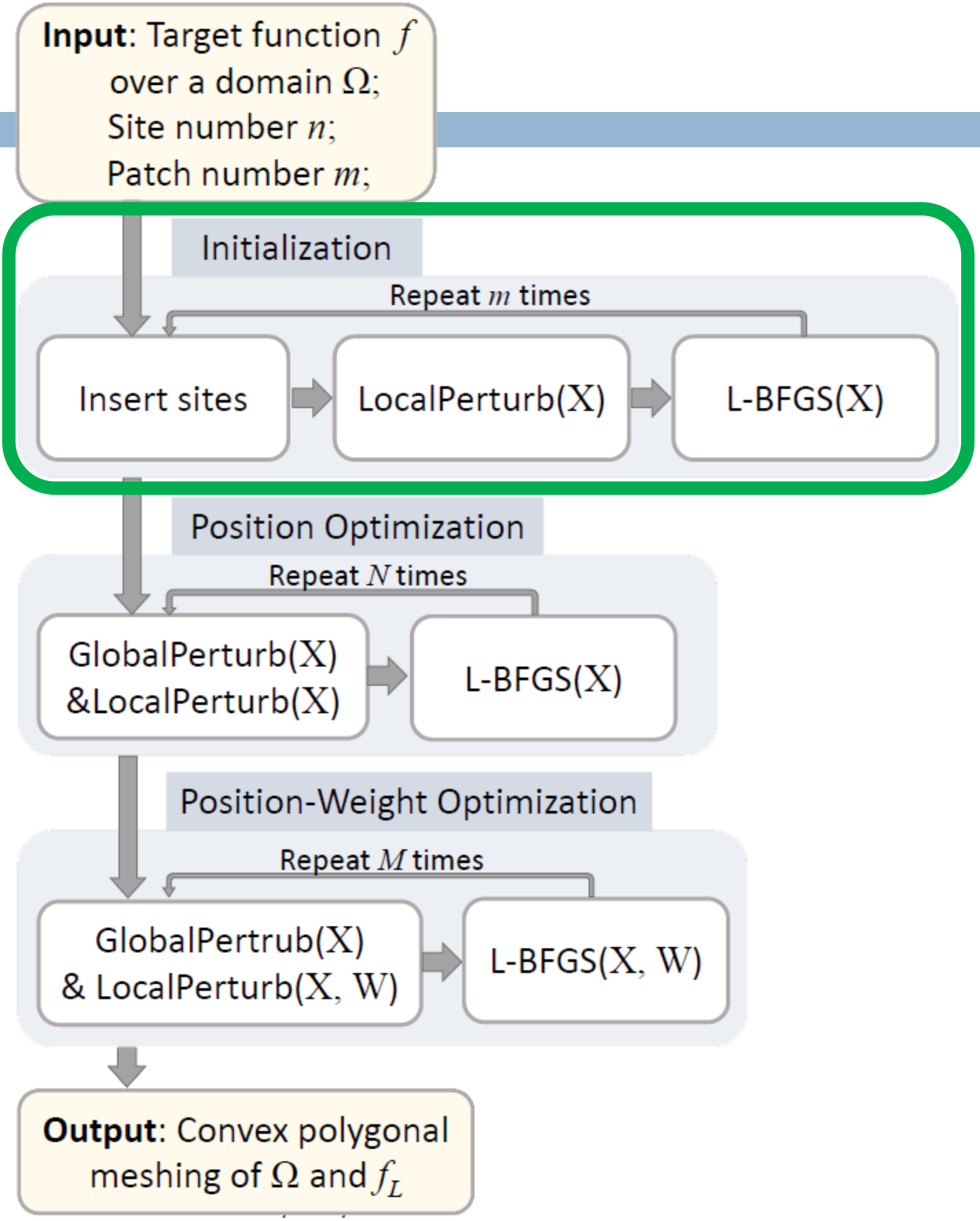

Optimization Framework

- Overview

(1) Initialization:

Insert and optimize site positions

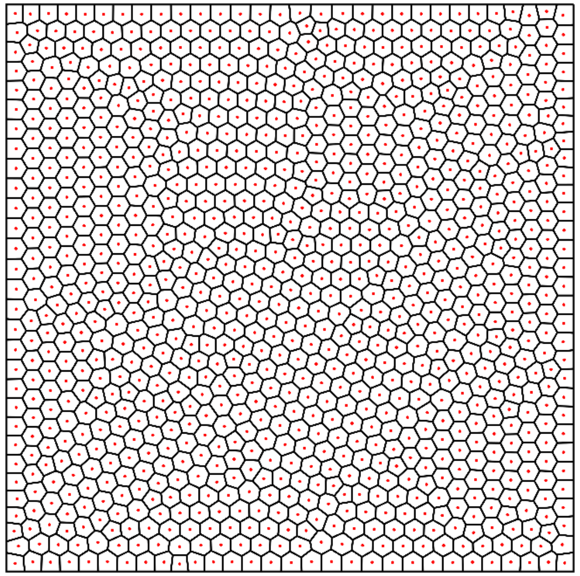

Random insertion

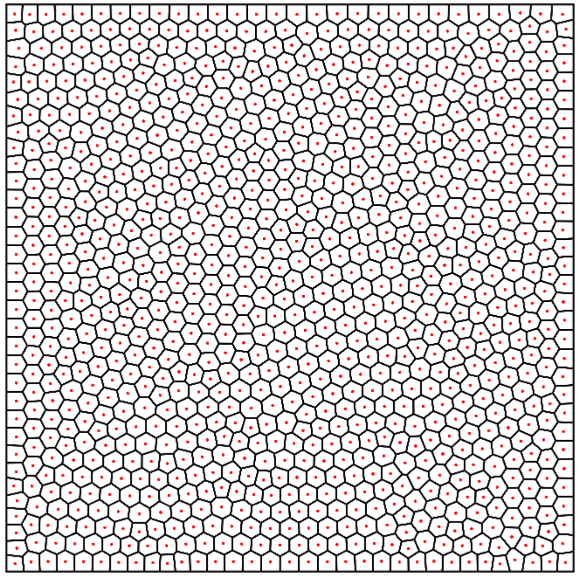

PCA-based insertion

$$f\left(x,y\right)=x^2+y^2$$

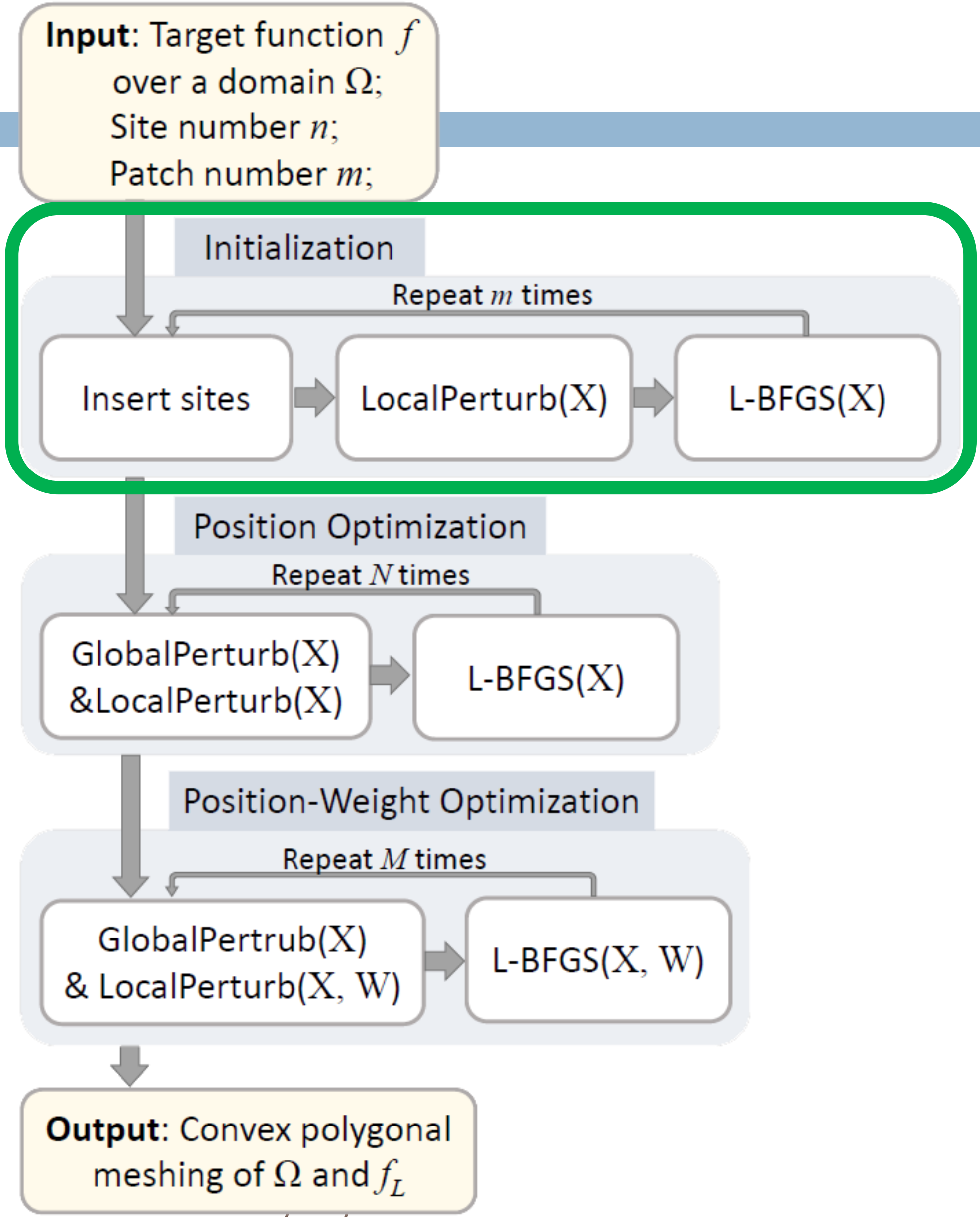

Optimization Framework

- Overview

(1) Initialization:
Insert and optimize site positions

(2) Position optimization:

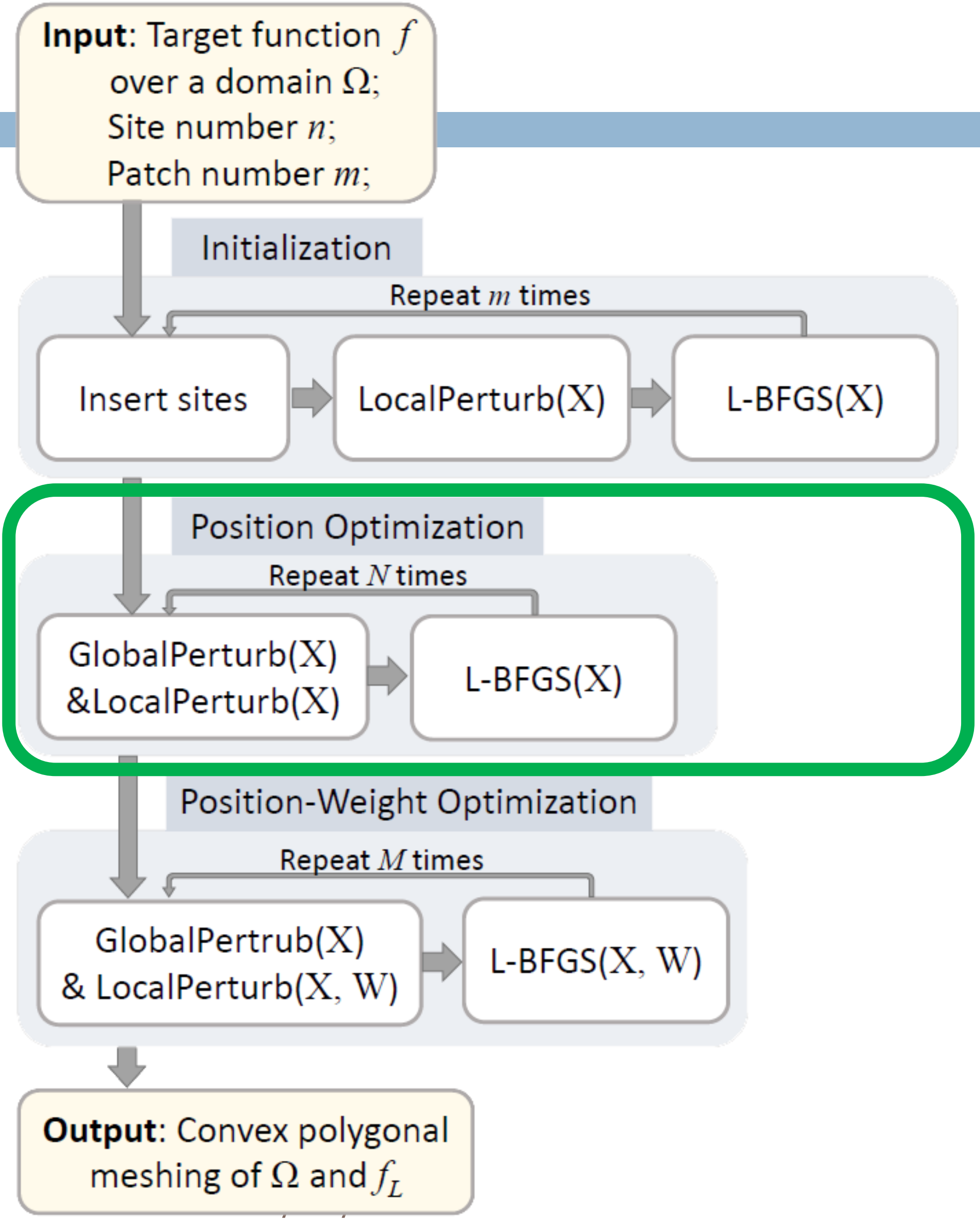

Optimization Framework

Overview

(1) Initialization:
Insert and optimize site positions

(2) Position optimization:

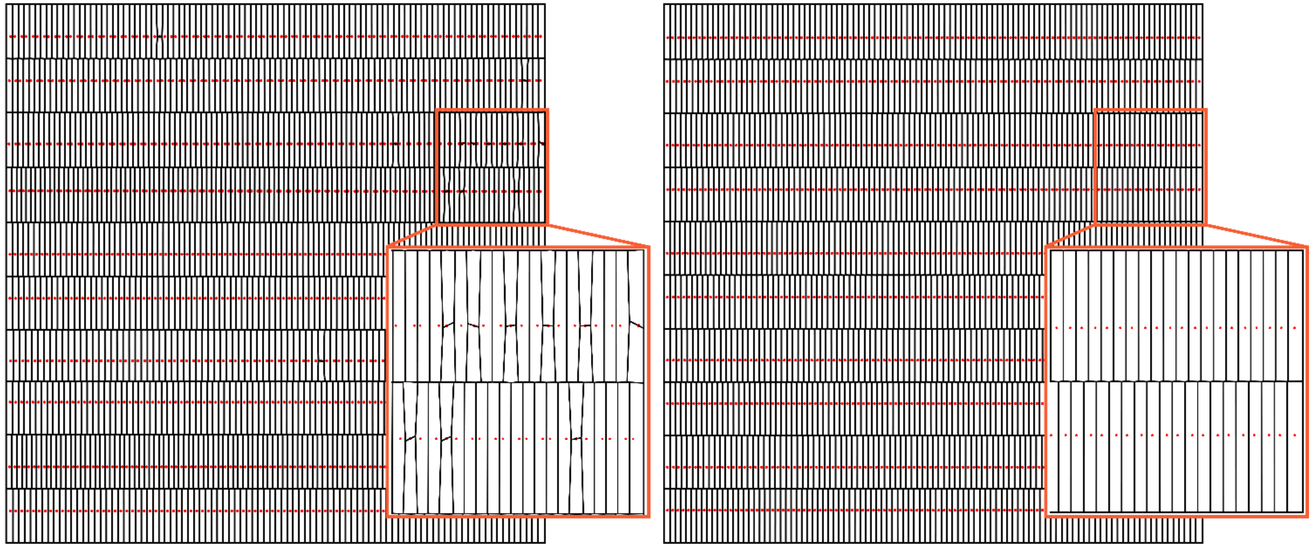

Local perturbation   Local&Global perturbation

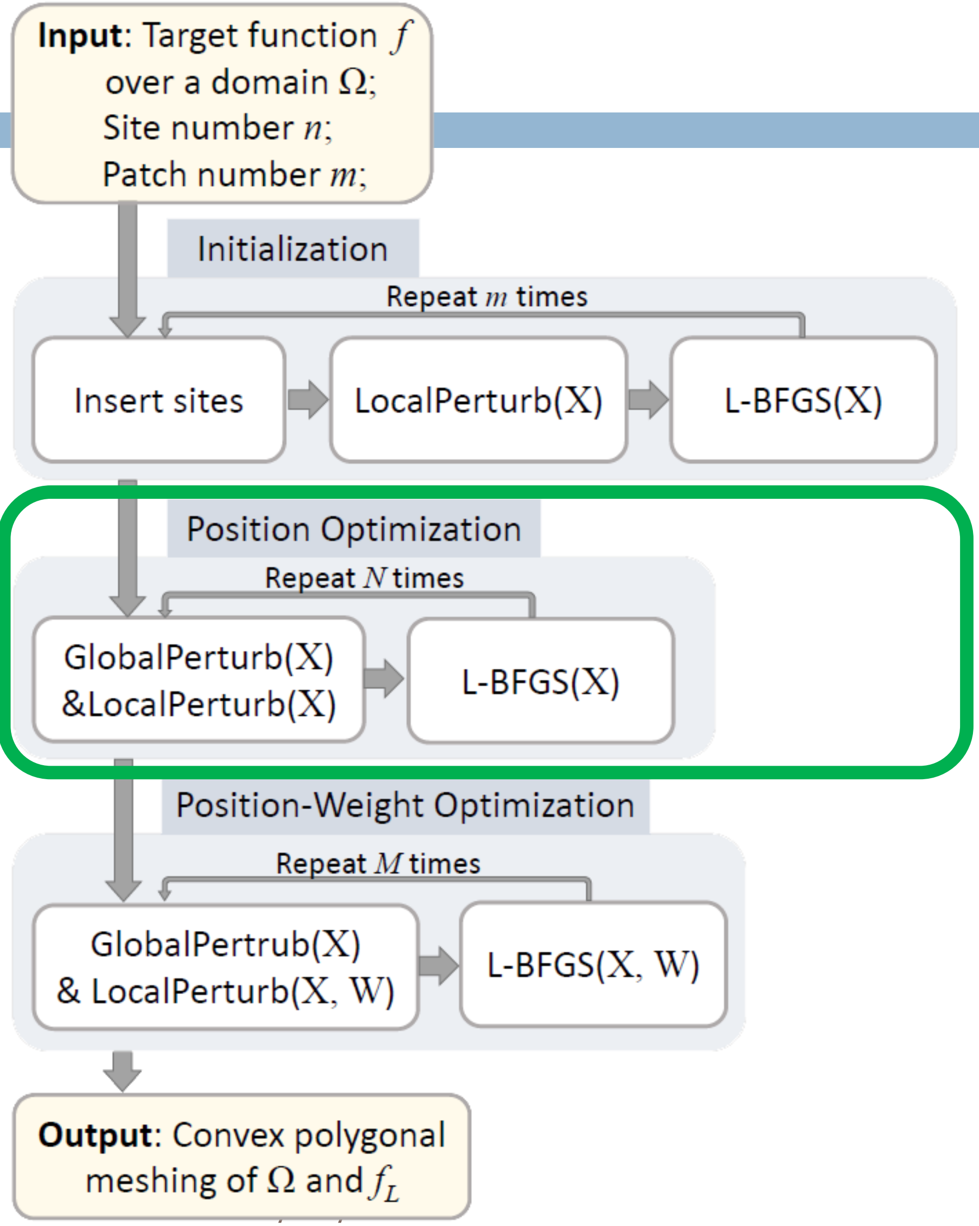

Optimization Framework

- Overview

(1) Initialization:
Insert and optimize site positions

(2) Position optimization:

(3) Position-weight optimization:

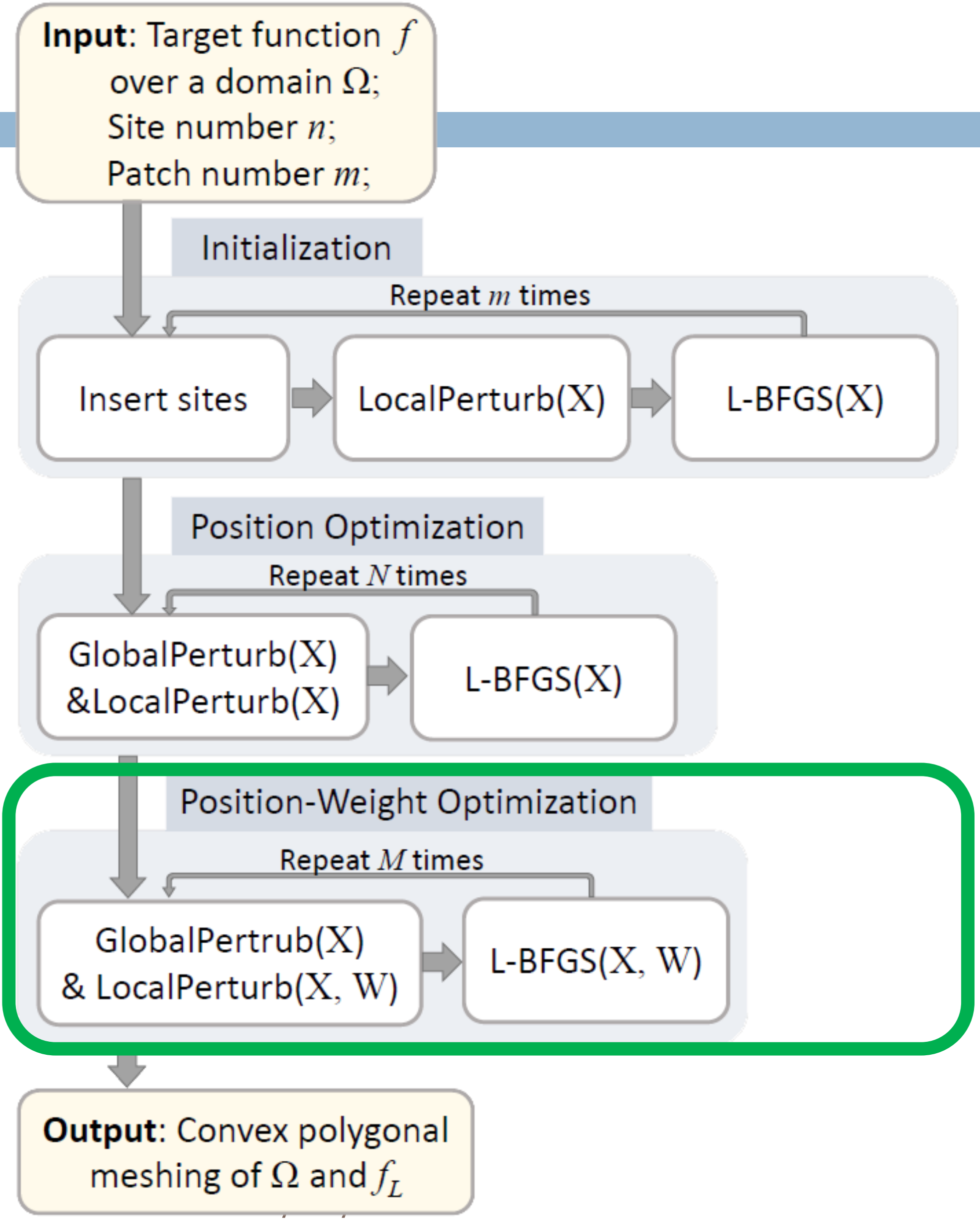

Optimization Framework

- Overview

(1) Initialization:
Insert and optimize site positions

(2) Position optimization:

(3) Position-weight optimization:

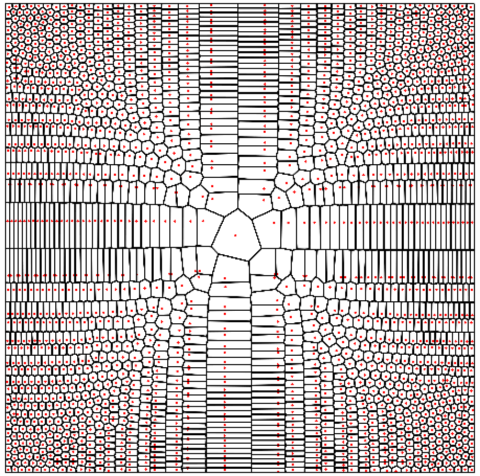

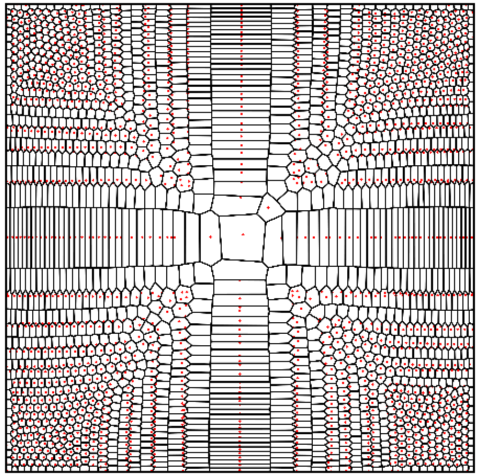

Position optimization result Position-weight optimization result

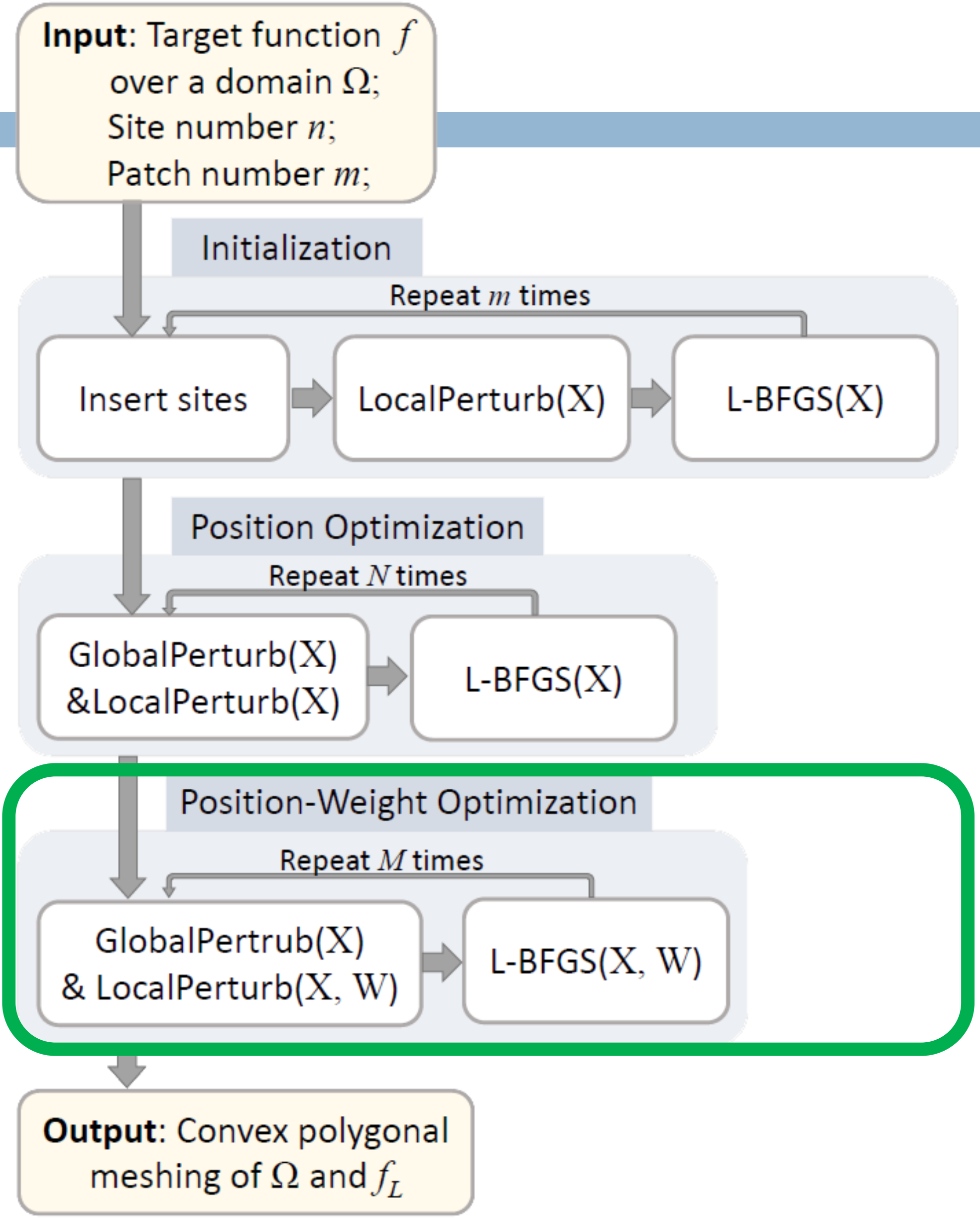

Results

- 1. Non-convex function approximation

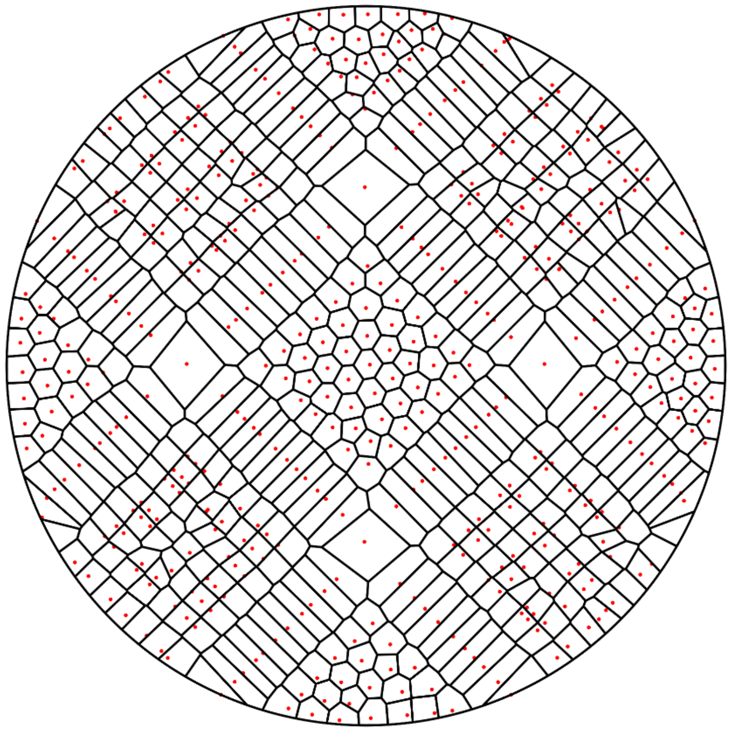

Resulting tessellation (left) and piecewise linear fit (right) of a non-convex target function $f(x, y) = \sin(\pi(x + 0.5))\cos(\pi y), x^2 + y^2 \leq 1$ with 500 sites

Results

- Density control

$\rho(x,y)=1.0$ $\rho(x,y)=1.0/\left(\left(x^2+y^2\right)^2+0.001\right)$

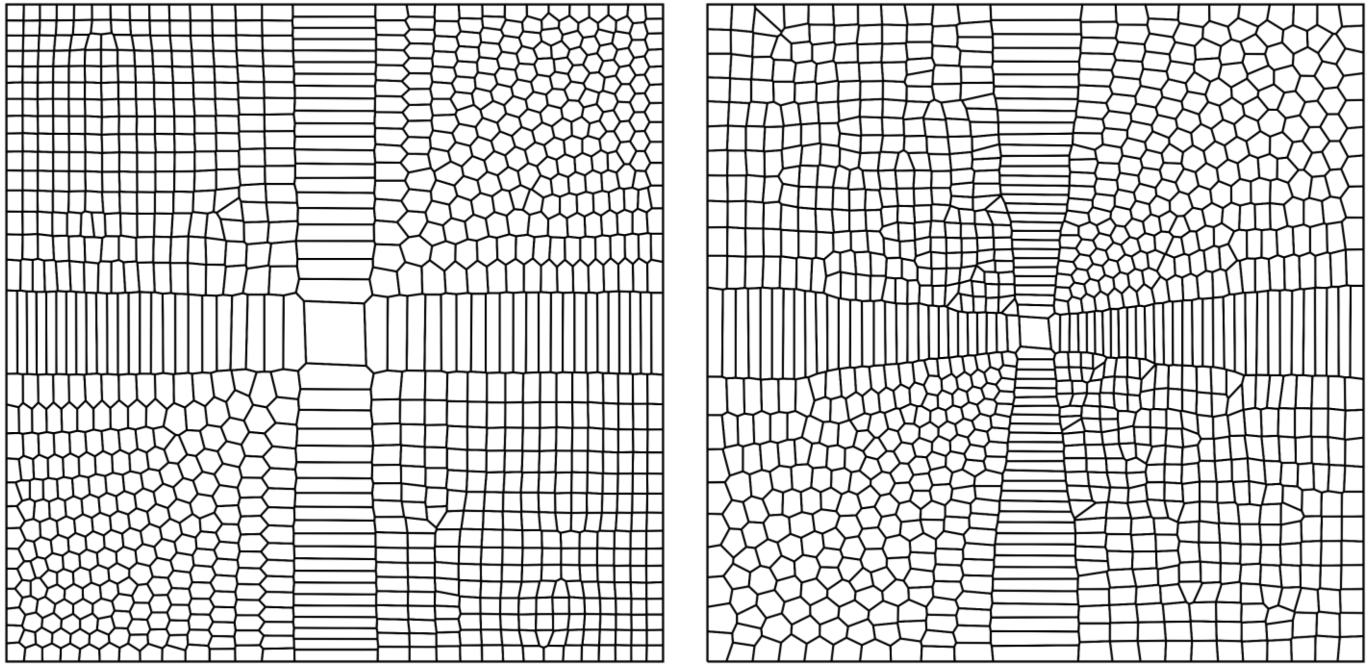

Resulting tessellations for a non-convex target function $f(x,y)=x^3+y^3, -1\le x,y\le 1$ with a constant density (left) and a non-uniform density function (right)

Results

- 3D results

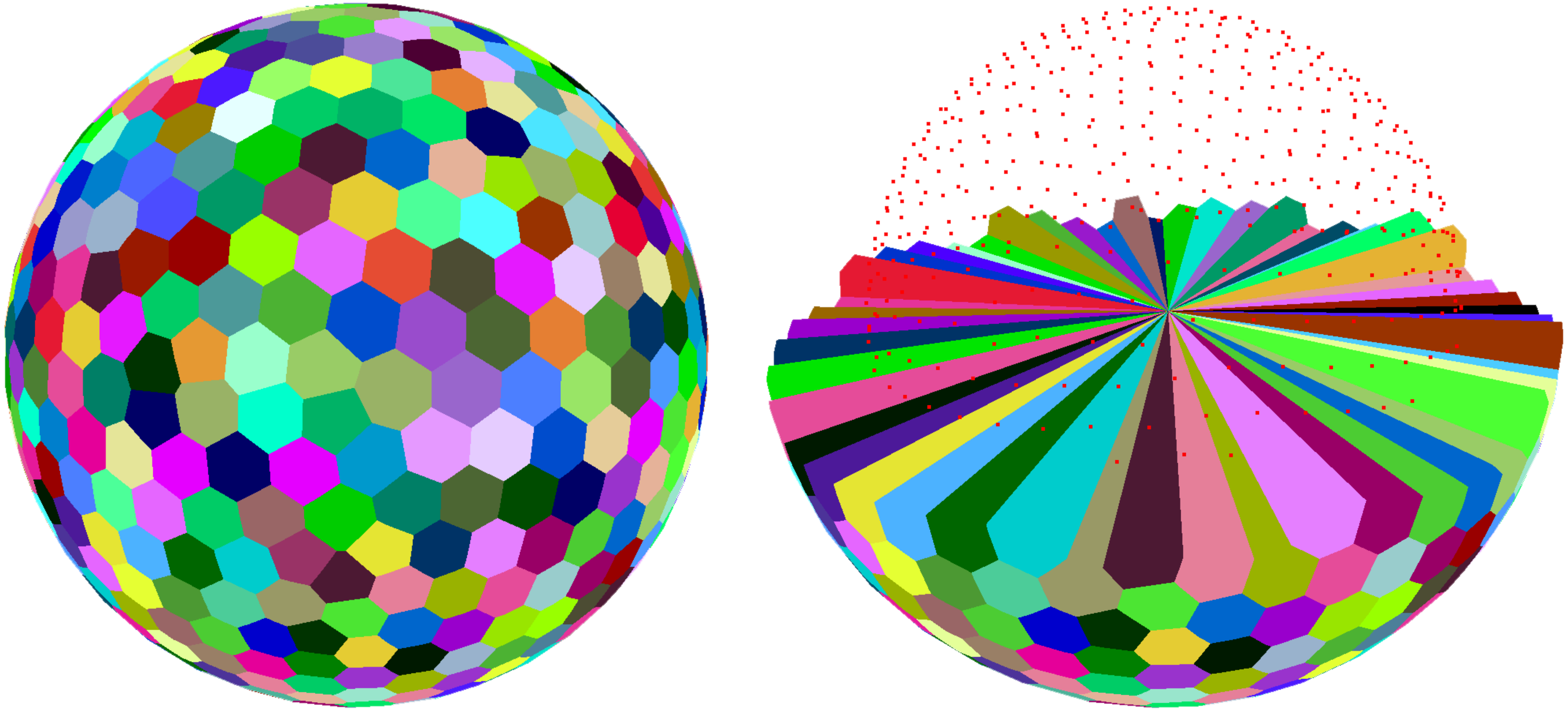

Tessellation of sphere for a non-smooth target function $f(x,y,z)=\sqrt{x^2+y^2+z^2}$ with 800 sites

Results

- 3D results

3D optimal power diagrams with increasing anisotropy
Left: isotropic, middle: 2:1:1, right: 8:1:1

Results

- 3D results

$$f\left(x,y,z\right)=x^{3}+y^{3}+z^{3},-1\le x,y,z\le 1$$

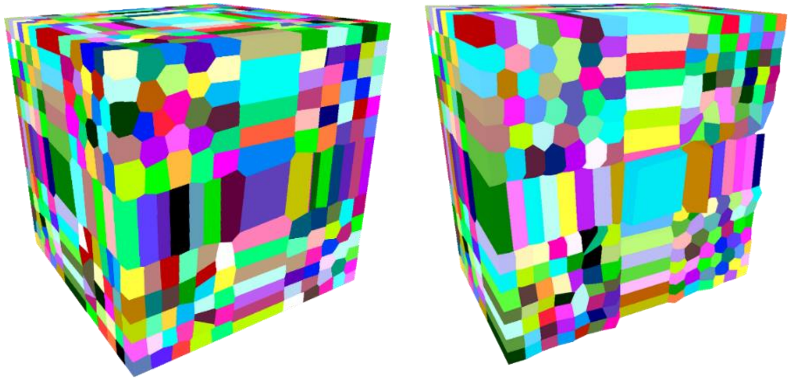

$$\rho\left(x,y,z\right)=1.0$$

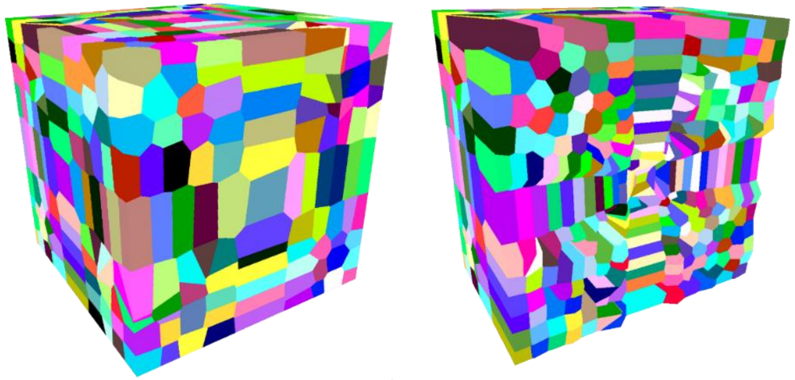

$$\rho\left(x,y,z\right)=1.0\Big/\left(\left(x^{2}+y^{2}+z^{2}\right)^{2}+0.001\right)$$

Exterior and cutaway views of tessellations for a non-convex target function with a constant density (top) and non-uniform density (bottom)

VII Applications

- Image approximation
- Surface approximation
- Point cloud resampling
- 3D printing
- Packing

Applications - Image Approximation

- Objective function:

$$E(X) = \sum_{i=1}^{N} \int_{\Omega_i} (|r(\mathbf{x}) - R_i^*(\mathbf{x})|^2 + |g(\mathbf{x}) - G_i^*(\mathbf{x})|^2 + |b(\mathbf{x}) - B_i^*(\mathbf{x})|^2) \mathrm{d}\mathbf{x},$$

Applications - Image Approximation

initialization

Applications - Image Approximation

after 10 iterations

Applications - Image Approximation

final result after 150 iterations

Applications - Surface Approximation [*CAGD'18*]

- Using generalized barycentric finite elements -- quadratic serendipity elements over planar polygons

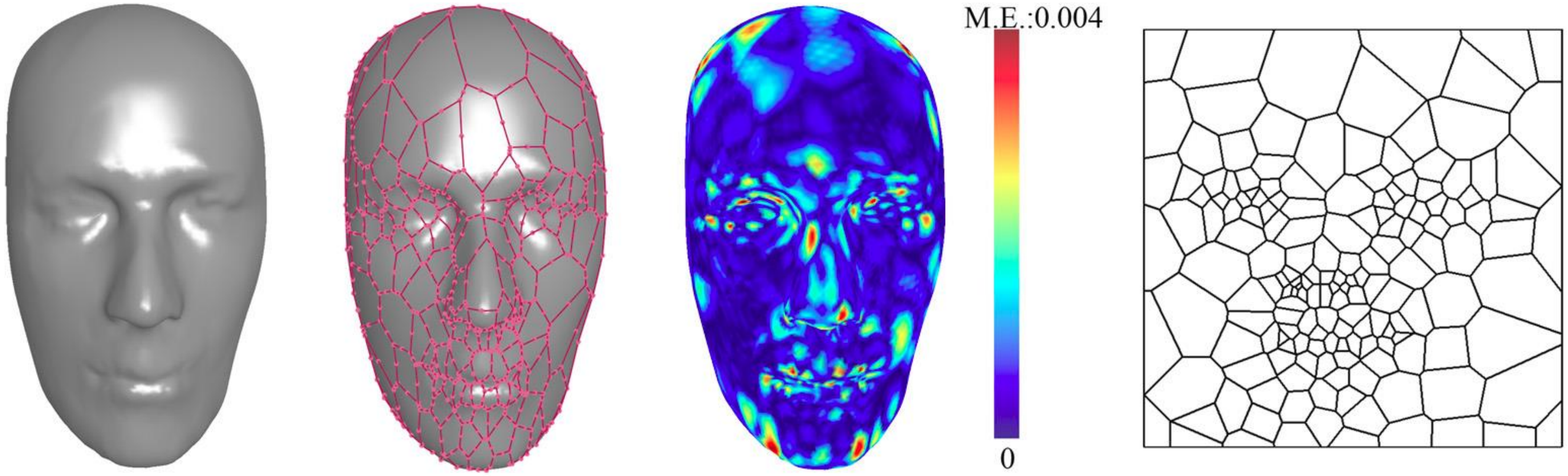

From left to right: the result surface, result surface with interpolated points, color-coded approximation errors, and the tessellation on the parametric domain.

Applications – Point Cloud Resampling*

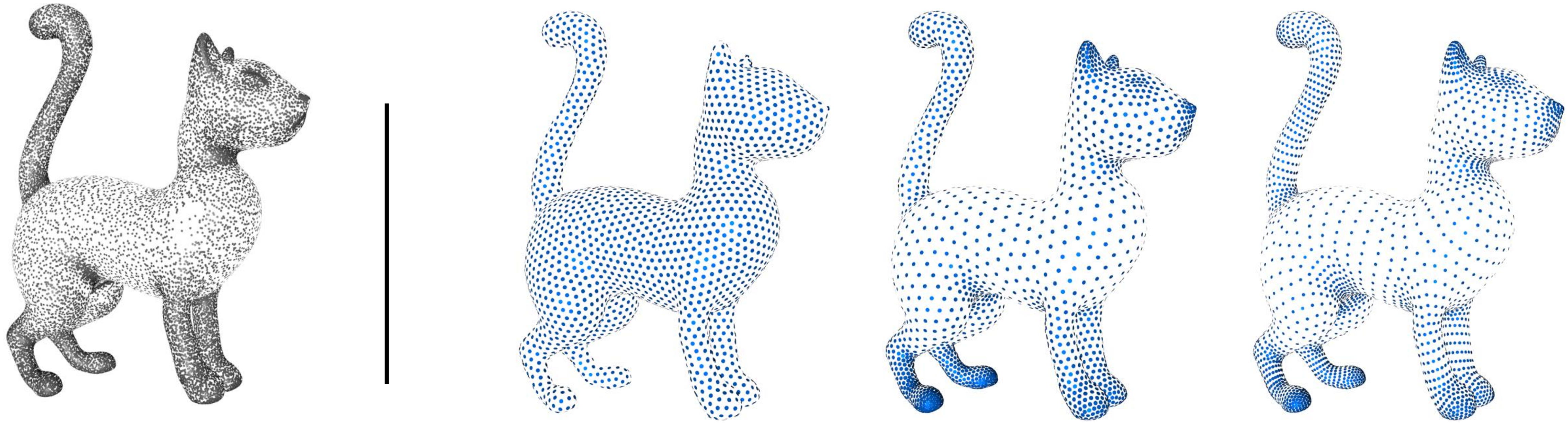

input point cloud output

*Zhonggui Chen, Tieyi Zhang, Juan Cao, Yongjie Jessica Zhang, Cheng Wang. Point Cloud Resampling Using Centroidal Voronoi Tessellation Methods. Computer-Aided Design (Proc. SPM), 102:12-21, 2018

Applications – Point Cloud Resampling

- Voronoi cells restricted on local fitting planes

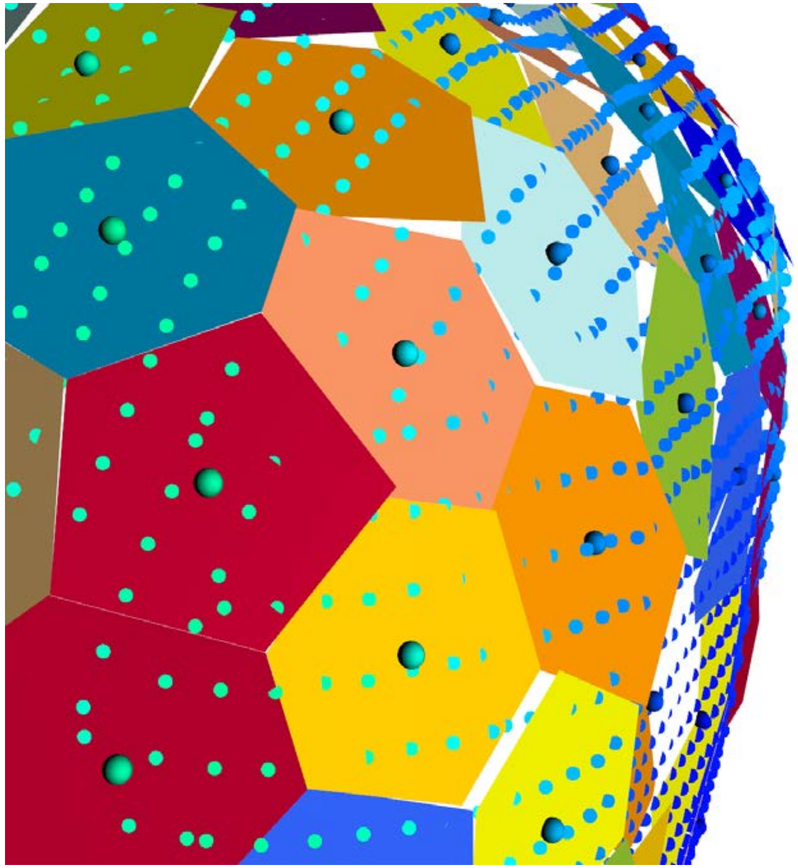

Applications – Point Cloud Resampling

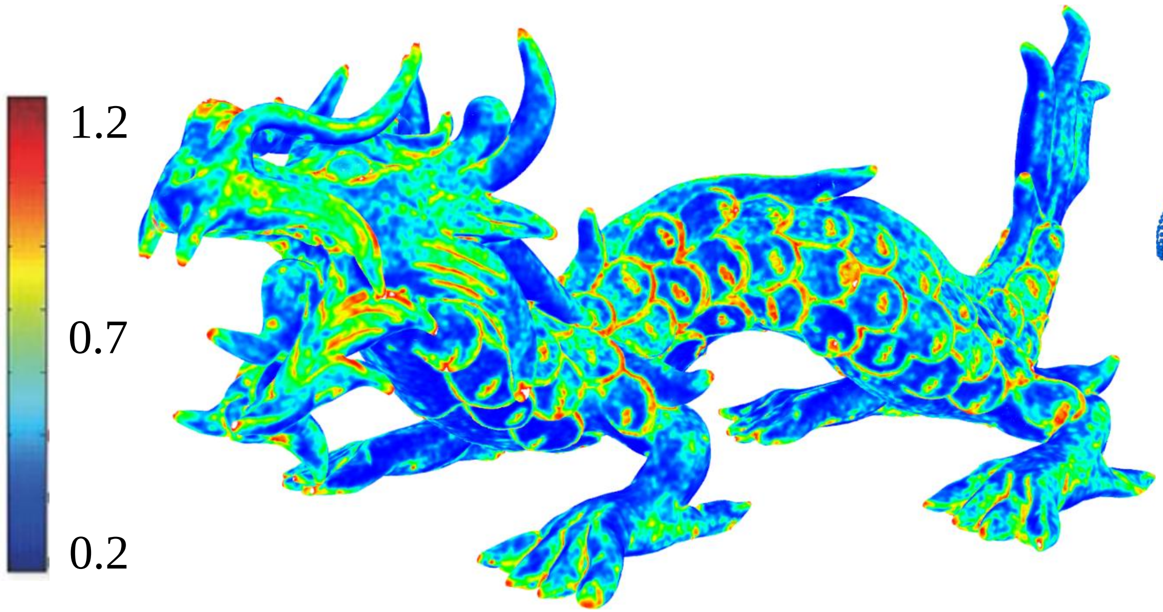

(a) input(3M)

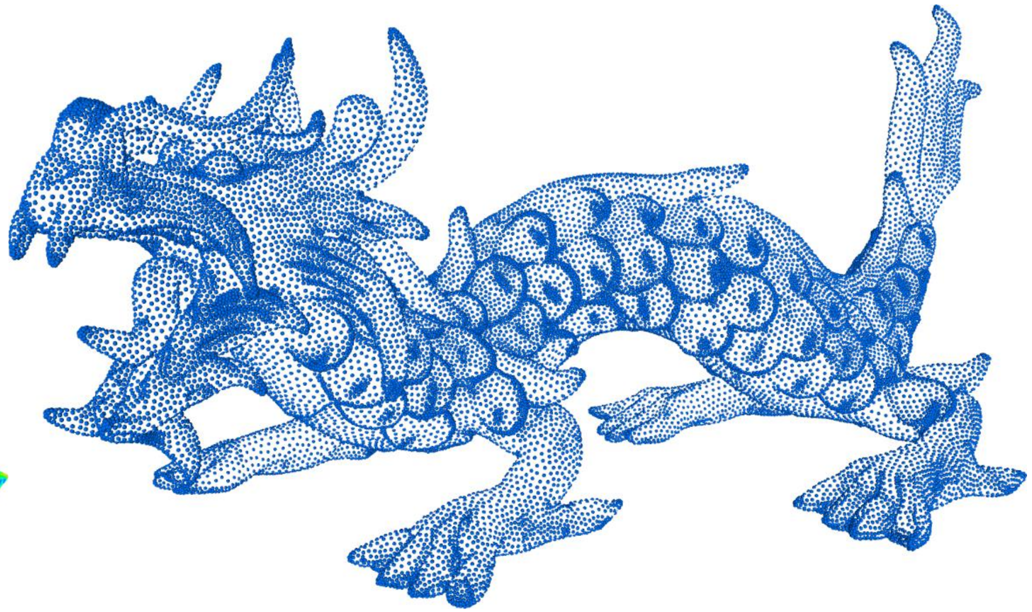

(b) weighted resampling(50k)

- *Adaptive resampling result* of scan data of a dragon model in 16.4s

Applications – Point Cloud Resampling

- *Running time* against the number of input points ranging from 10K to 10M, with a fixed output point number (m = 10K)

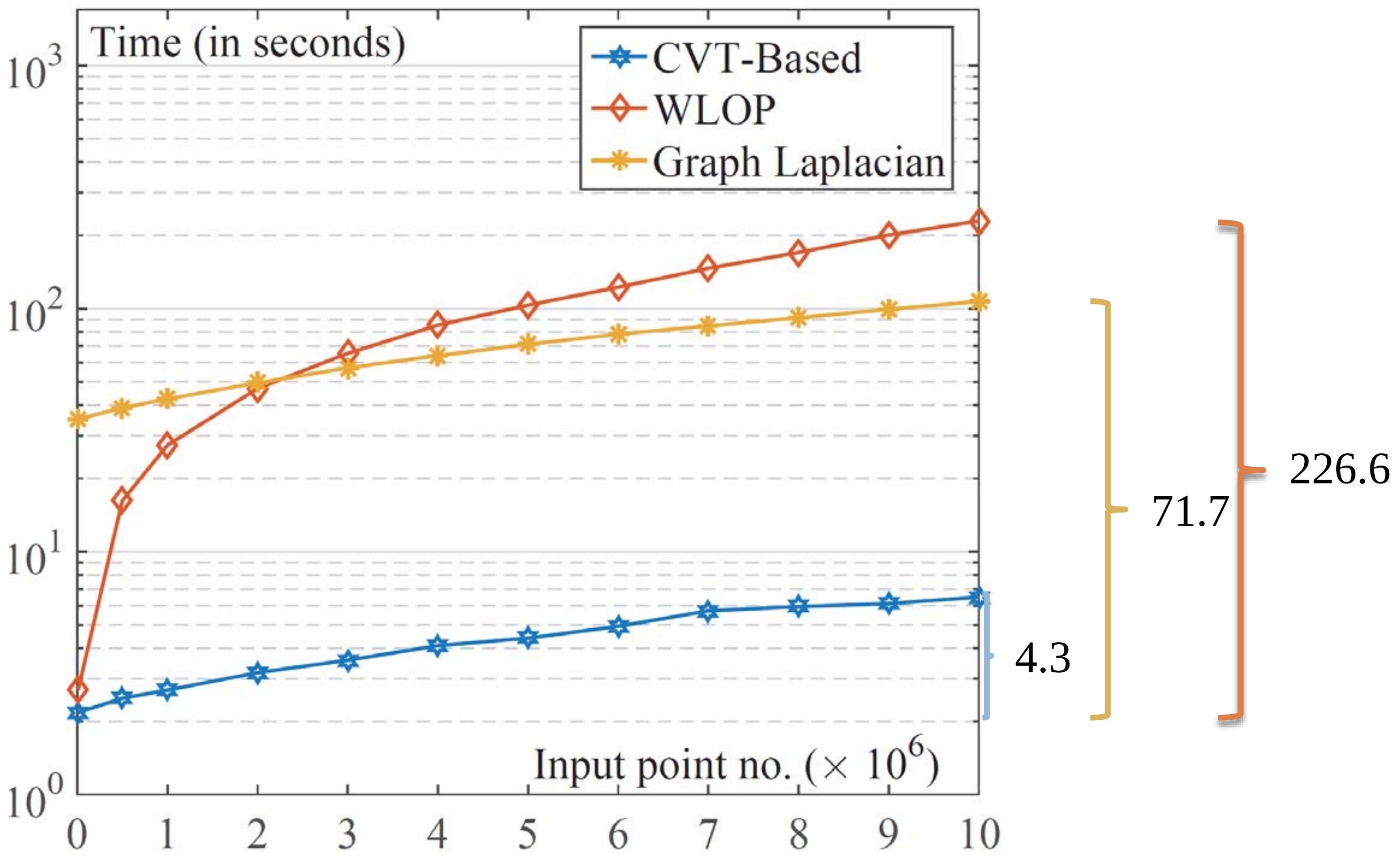

Applications – 3D Printing [*Computers & Graphics'17*]

- Line Drawing for 3D Printing

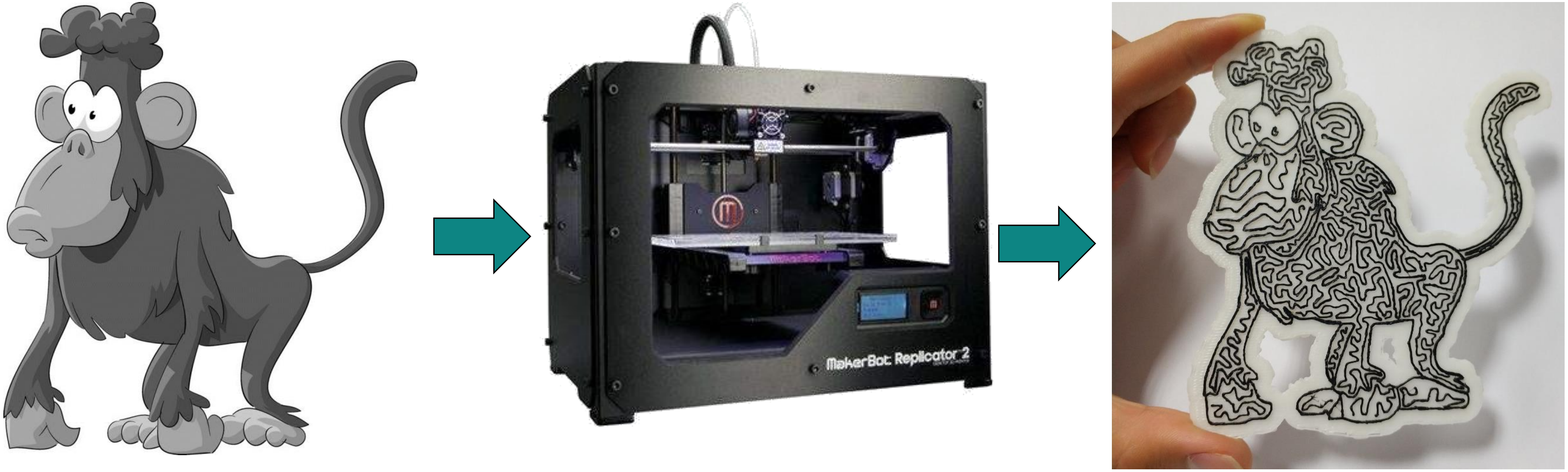

Applications – 3D Printing

- Algorithm overview

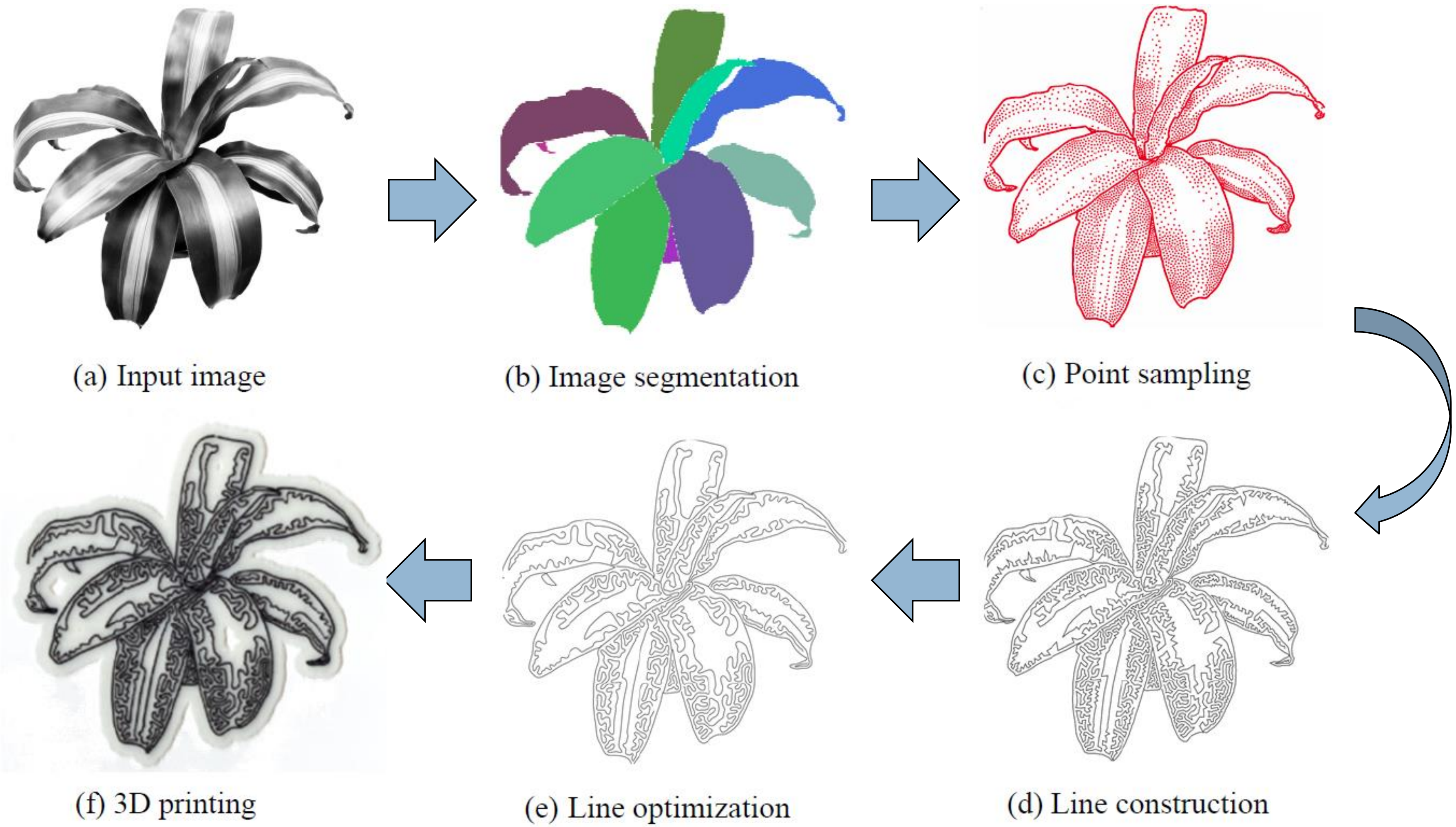

Applications – 3D Printing

- Printing results

Applications – Irregular Packing [*TVCG'16*]

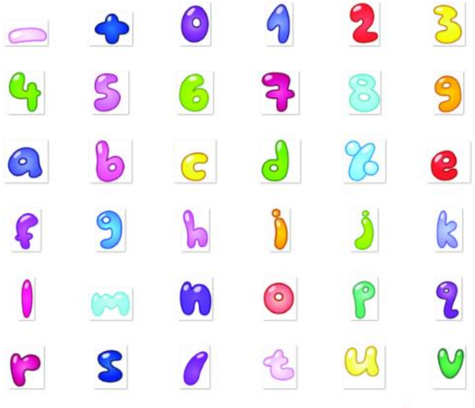

Tiles

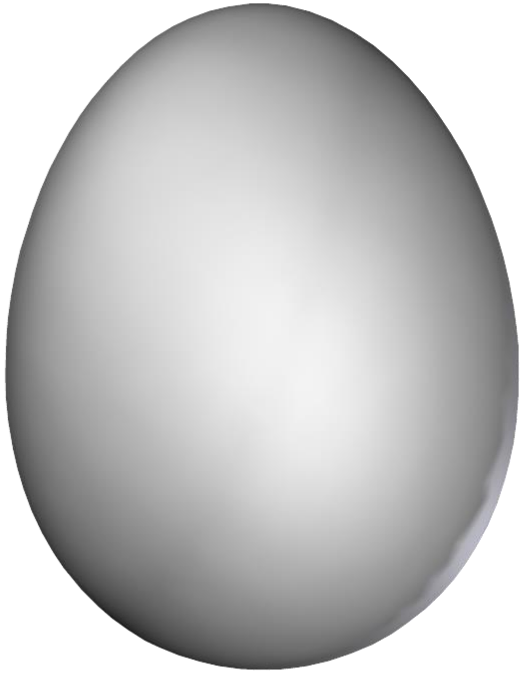

Surface

Decorated Surface

Input

Output

Applications – Irregular Packing

- Iterative Relaxation Method
  - **Surface Partitioning**: divide the supporting surface into a set of nonoverlapping regions
  - **Tile Optimization**: adjust the orientation, location and scaling of each tile

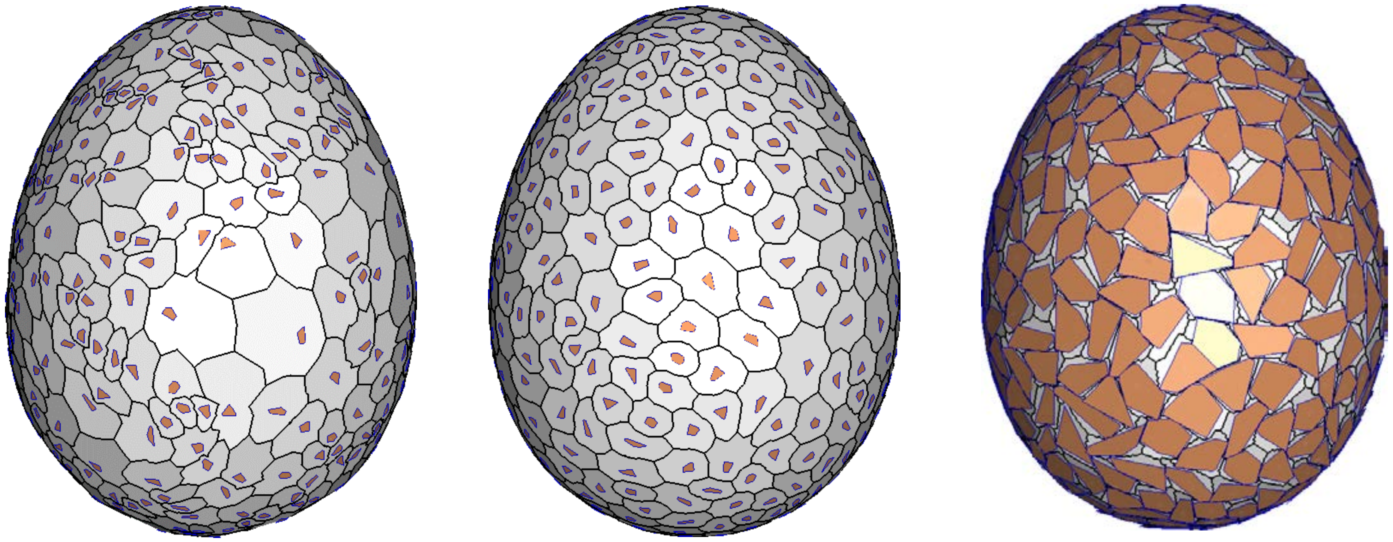

Initial placement After one iteration After convergence

Applications – Irregular Packing

- Packing irregular tiles on surfaces



Applications – Irregular Packing

- Packing irregular 3D shapes [*SGP'18*]

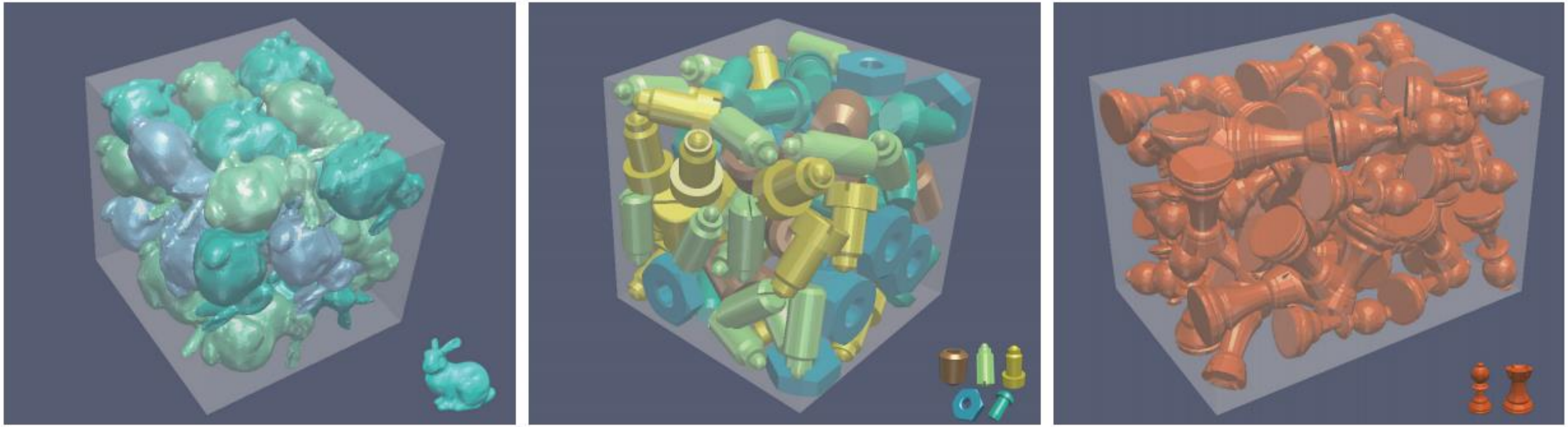

Summary and Future Work

- Variational principle for optimal tessellation generation
- Piecewise approximation problems
  - Basis functions
  - Tessellations
- Efficient optimization methods
- Applications

References

- Yuexin Ma, Zhonggui Chen, Wenchao Hu, Wenping Wang. **Packing Irregular Objects in 3D Space via Hybrid Optimization**. Computer Graphics Forum (Proc. SGP), 37(5):49-59, 2018
- Yanyang Xiao, Zhonggui Chen, Juan Cao, Yongjie Jessica Zhang, Cheng Wang. **Optimal Power Diagrams via Function Approximation**. Computer-Aided Design (Proc. SPM; Best Paper Award 1st Place), 102:52-60, 2018
- Zhonggui Chen, Tieyi Zhang, Juan Cao, Yongjie Jessica Zhang, Cheng Wang. **Point Cloud Resampling Using Centroidal Voronoi Tessellation Methods**. Computer-Aided Design (Proc. SPM), 102:12-21, 2018
- Juan Cao, Yanyang Xiao, Zhonggui Chen, Wenping Wang, Chandrajit Bajaj. **Functional Data Approximation on Bounded Domains using Polygonal Finite Elements**. Computer Aided Geometric Design, 63:149–163, 2018
- Zhonggui Chen, Zifu Shen, Jianzhi Guo, Juan Cao, Xiaoming Zeng. **Line Drawing for 3D Printing**. Computers & Graphics (Proc. SMI), 66: 85-92, 2017
- Saifeng Ni, Zichun Zhong, Yang Liu, Wenping Wang, Zhonggui Chen and Xiaohu Guo. **Sliver-Suppressing Tetrahedral Mesh Optimization with Gradient-Based Shape Matching Energy**. Computer Aided Geometric Design (Proc. GMP), 52–53:247-261, 2017
- Shiqin Xin, Bruno Lévy, Zhonggui Chen, Lei Chu, Yaohui Yue, Wenping Wang. **Centroidal power diagrams with capacity constraints: computation, applications, and extension**. ACM Transactions on Graphics, 2016, 35(6):1-12.
- Wenchao Hu, Zhonggui Chen, Hao Pan, Yizhou Yu, Eitan Grinspun, Wenping Wang**. Surface Mosaic Synthesis with Irregular Tiles**. IEEE Transactions on Visualization and Computer Graphics, 22(3):1302-1313, 2016
- Zhonggui Chen, Wenping Wang, Bruno Lévy, Ligang Liu, Feng Sun. **Revisiting Optimal Delaunay Triangulation for 3D Graded Mesh Generation**. SIAM Journal on Scientific Computing, 36(3), A930-A954, 2014
- Zhonggui Chen, Yanyang Xiao, Juan Cao. **Approximation by Piecewise polynomials on Voronoi Tessellation**. Graphical Models (Proc. GMP 2014), 76(5), 522-531, 2014
- Zhonggui Chen, Zhan Yuan, Yi-King Choi, Ligang Liu, Wenping Wang. **Variational Blue Noise Sampling**, IEEE Transactions on Visualization and Computer Graphics, 18(10): 1784- 1796, 2012
- Zhonggui Chen, Juan Cao, Wenping Wang. **Isotropic Surface Remeshing Using Constrained Centroidal Delaunay Mesh**, Computer Graphics Forum,31(7):2077–2085, 2012

THE END